Astronomy & Astrophysics manuscript no. aluminium˙I˙and˙II˙copy
December 8, 2020
© ESO 2020

arXiv:1808.09478v1 [physics.atom-ph] 28 Aug 2018

Extended transition rates and lifetimes in Al I and Al II from systematic multiconfiguration calculations

A. Papoulia[1,2], J. Ekman[1], and P. Jönsson[1]

[1] Materials Science and Applied Mathematics, Malmö University, SE-20506 Malmö, Sweden
e-mail: asimina.papoulia@mau.se
[2] Division of Mathematical Physics, Lund University, Post Office Box 118, SE-22100 Lund, Sweden

Received -, 2018;

ABSTRACT

Aims. The objective of this work is to provide a substantial amount of updated atomic data for the systems of neutral and singly ionized aluminium, including transition data in the infrared region. This is particularly important since the new generation of telescopes are designed for this region.

Methods. Multiconfiguration Dirac-Hartree-Fock (MCDHF) and relativistic configuration interaction (RCI) calculations were performed for 28 and 78 states in neutral and singly ionized aluminium, respectively. In Al I, the configurations of interest are $3s^2nl$ for $n = 3, 4, 5$ with $l = 0$ to 4, as well as $3s3p^2$ and $3s^26l$ for $l = 0, 1, 2$. In Al II, the studied configurations are, besides the ground configuration $3s^2$, $3snl$ with $n = 3$ to 6 and $l = 0$ to 5, $3p^2$, $3s7s$, $3s7p$ and $3p3d$. Valence and core-valence electron correlation effects are systematically accounted for through large configuration state function (CSF) expansions.

Results. Calculated excitation energies are found to be in excellent agreement with experimental data from the NIST database. Lifetimes and transition data for radiative electric dipole (E1) transitions are given and compared with results from previous calculations and available measurements, for both Al I and Al II. The computed lifetimes of Al I are in very good agreement with the measured lifetimes in high-precision laser spectroscopy experiments. There is a significant improvement in accuracy, in particular for the more complex system of neutral Al I.

Key words. atomic data

1. Introduction

Aluminium is an important element in astrophysics. In newly born stars the galactic [Al/H] abundance ratio, as well as the [Al/Mg] ratio are found to be increased in comparison to early stars (Clayton 2003). The aluminium abundance and its anti-correlation with the one of magnesium is the best tool to determine which generation a globular cluster star belongs to. The abundance variations of different elements and the relative numbers of first and second generation stars may be used to determine the nature of polluting stars, the timescale of the star formation episodes and the initial mass function of the stellar cluster (Carretta et al. 2010). The aluminium abundance is of importance for other types and groups of stars as well. A large number of spectral lines of neutral and singly ionized aluminium are observed in the solar spectrum and in many stellar spectra. Aluminium is one of the interesting elements for chemical analysis of the Milky Way and one example is the Gaia-ESO Survey[1], in which medium- and high-resolution spectra from more than 10^5 stars are analyzed to provide public catalogs with astrophysical parameters. As part of this survey, Smiljanic et al. (2014) analyzed high-resolution UVES[2] spectra of FGK-type stars and derived abundances for 24 elements, including aluminium.

In addition, aluminium abundances have been determined in local disk and halo stars by Gehren et al. (2004), Reddy et al. (2006), Mishenina et al. (2008), Adibekyan et al. (2012) and Bensby et al. (2014). However, chemical evolution models still have problems reproducing the observed behavior of the aluminium abundance in relation to abundances of other elements. Such examples are the observed trends of the aluminium abundances in relation to metallicity [Fe/H], which are not well reproduced at the surfaces of stars, like giants and dwarfs (Smiljanic et al. 2016). On grounds of the above issues, Smiljanic et al. (2016) redetermined aluminium abundances within the Gaia-ESO Survey. Furthermore, strong deviations from local thermodynamic equilibrium (LTE) are found to significantly affect the inferred aluminium abundances in metal poor stars, which was highlighted in the work by Gehren et al. (2006). Nordlander and Lind (2017) presented a non-local thermodynamic equilibrium (NLTE) modeling of aluminium and provided abundance corrections for lines in the optical and near-infrared regions.

Correct deduction of aluminium abundances and chemical evolution modeling is thus necessary to put together a complete picture of the stellar and Galactic evolution. Obtaining the spectroscopic reference data to achieve this goal is demanding. Significant amount of experimental research has been conducted to probe the spectra of Al II and Al I and facilitate the analysis of the astrophysical observations. Yet, some laboratory measurements still lack reliability and in many cases, especially when going to higher excitation energies, only theoretical values of transition properties exist. Accurate computed atomic data are therefore essential to make abundance analyses in the Sun and other stars possible.

[1] http://casu.ast.cam.ac.uk/surveys-projects/ges
[2] http://www.eso.org/sci/facilities/paranal/instruments/uves.html

For the singly ionized Al II, there is a number of measurements of transition properties. The radiative lifetime of the $3s3p\ ^3P^o_1$ level was measured by Johnson et al. (1986) using an ion storage technique and the transition rate value for the inter-combination $3s3p\ ^3P^o_1 \rightarrow 3s^2\ ^1S_0$ transition was provided. Träbert et al. (1999) measured lifetimes in an ion storage ring and the result for the lifetime of the $3s3p\ ^3P^o_1$ level is in excellent agreement with the one measured by Johnson et al. (1986). Using the beam-foil technique, Andersen et al. (1971) measured lifetimes for the $3snf\ ^3F$ series with $n = 4 - 7$, although those measurements are associated with significant uncertainties. By using the same technique, the lifetime of the singlet $3s3p\ ^1P^o_1$ level was measured in four different experimental works (Kernahan et al. 1979; Head et al. 1976; Berry et al. 1970; Smith 1970), which are in very good agreement.

In the case of neutral Al I, several measurements have also been performed. Following a sequence of earlier works (Jönsson and Lundberg 1983; Jönsson et al. 1984), Buurman et al. (1986) used laser spectroscopy to obtain experimental values for the oscillator strengths of the lowest part of the spectrum. A few years later, Buurman and Dönszelmann (1990) redetermined the lifetime of the $3s^24p\ ^2P$ level and separated the different fine-structure components. Using similar laser techniques, Davidson et al. (1990) measured the natural lifetimes of the $3s^2nd\ ^2D$ Rydberg series and obtained oscillator strengths for transitions to the ground state. In a more recent work, Vujnović et al. (2002) used the hollow cathode discharge method to measure relative intensities of spectral lines of both neutral and singly ionized aluminium. Absolute transition probabilities were evaluated based on available results from previous studies, such as the ones mentioned above.

Al II is a nominal two-electron system and the lower part of its spectrum is strongly influenced by the interaction between the $3s3d\ ^1D$ and $3p^2\ ^1D$ configuration states. Contrary to neutral Mg I where no level is classified as $3p^2\ ^1D$, in Al II the $3p^2$ configuration dominates the lowest ^1D term and yields a well-localized state below the $3s3d\ ^1D$ term. The interactions between the $3snd\ ^1D$ Rydberg series and the $3p^2\ ^1D$ perturber were investigated by Tayal and Hibbert (1984). Going slightly further up, the spectrum of Al II is governed by the strong mixing of the $3snf\ ^3F$ Rydberg series with the $3p3d\ ^3F$ term. Despite the widespread mixing, $3p3d\ ^3F$ is also localized, between the $3s6f\ ^3F$ and $3s7f\ ^3F$ states. The configuration interaction between doubly excited states, e.g. the $3p^2\ ^1D$ and $3p3d\ ^3F$ states, and singly excited $3snl\ ^{1,3}L$ states was thoroughly investigated by Chang and Wang (1987). However, the extreme mixing of the $3p3d\ ^3F$ term in the $3snf\ ^3F$ series and its effect on the computation of transition properties was first investigated by Weiss (1974). Although the work by Chang and Wang (1987) was more of a qualitative nature, computed transition data were provided based on configuration interaction (CI) calculations. Using the B-spline configuration interaction (BSCI) method, Chang and Fang (1995) also predicted transition properties, as well as lifetimes of Al II excited states.

Despite the large number of measured spectral lines in Al I, the $3s3p^2\ ^2D$ state could not be experimentally identified and for a long time theoretical calculations had been trying to localize it and predict whether it lies above or below the first-ionization limit. Al I is a system with three valence electrons and correlation effects are even stronger compared to the singly ionized Al II. Especially strong is the two-electron interaction of $3s3d\ ^1D$ with $3p^2\ ^1D$, which becomes evident between the $3s^23d\ ^2D$ and $3s3p^2\ ^2D$ states. The $3s3p^2\ ^2D$ state is strongly coupled to the $3s^23d\ ^2D$ state, but it is also smeared out over the entire discrete part of the $3s^2nd\ ^2D$ series and contributes to a significant mixing of all those states (Weiss 1974). Asking for the position of the $3s3p^2\ ^2D$ level is thus meaningless, since it does not correspond to any single spectral line (Lin 1974; Trefftz 1988). Due to this strong two-electron interaction, the line strength of one of the ^2D states involved in a transition appears to be enhanced, while the line strength of the other ^2D state is being suppressed. This makes the computation of transition properties in Al I far from trivial (Froese Fischer et al. 2006). More theoretical studies on the system of neutral aluminium were conducted by Taylor et al. (1988) and Theodosiou (1992).

In view of the great astrophysical interest for accurate atomic data, close coupling (CC) calculations were carried out for the systems of Al II and Al I, by Butler et al. (1993) and Mendoza et al. (1995), respectively, as part of the Opacity Project. These extended spectrum calculations produced transition data in the infrared region (IR), which were scarce until then. However, the neglected relativistic effects, as well as the insufficient amount of correlation included in the calculations constitute limiting factors to the accuracy of the results. Later on, Froese Fischer et al. (2006) performed multiconfiguration Hartree-Fock (MCHF) calculations and used the Breit-Pauli (BP) approximation to also capture relativistic effects for Mg- and Al-like sequences. Focusing more on correlation, relativistic effects were kept to lower order. Even so, in Al I, correlation in the core and core-valence effects were not included due to limited computational resources. The latest compilation of Al II and Al I transition probabilities was made available by Kelleher and Podobedova (2008a). Wiese and Martin (1980) had earlier updated the first critical compilation of atomic data by Wiese et al. (1969).

Although for the past decades a considerable amount of research has been conducted for the systems of Al II and Al I, there is still a need for extended and accurate theoretical transition data. The present study is motivated by such a need. To obtain energy separations and transition data, the fully relativistic multiconfiguration Dirac-Hartree-Fock (MCDHF) scheme has been employed. Valence and core-valence electron correlation is included in the computations of both systems. Spectrum calculations have been performed to include the first 28 and 78 lowest states in neutral and singly ionized aluminium, respectively. Transition data corresponding to IR lines have also been produced. The excellent description of energy separations is an indication of highly accurate computed atomic properties, which can be used to improve the interpretation of abundances in stars.

2. Theory

2.1. Multiconfiguration Dirac-Hartree-Fock

The wave functions describing the states of the atom, referred to as atomic state functions (ASFs), are obtained by applying the multiconfiguration Dirac-Hartree-Fock approach (MCDHF) (Grant 2007; Froese Fischer et al. 2016). In the MCDHF method, the ASFs are approximate eigenfunctions of the Dirac-Coulomb Hamiltonian given by

$$H_{DC} = \sum_{i=1}^{N}[c\ \boldsymbol{\alpha}_i \cdot \mathbf{p}_i + (\beta_i - 1)c^2 + V_{nuc}(r_i)] + \sum_{i<j}^{N} \frac{1}{r_{ij}}, \qquad (1)$$

where $V_{nuc}(r_i)$ is the potential from an extended nuclear charge distribution, $\boldsymbol{\alpha}$ and β are the 4×4 Dirac matrices, c the speed of light in atomic units and $\mathbf{p} \equiv -\mathrm{i}\nabla$ the electron momentum operator. An ASF $\Psi(\gamma PJM_J)$ is given as an expansion over N_{CSF}

configuration state functions (CSFs), $\Phi(\gamma_i PJM_J)$, characterized by total angular momentum J and parity P:

$$\Psi(\gamma PJM_J) = \sum_{i=1}^{N_{CSF}} c_i \Phi(\gamma_i PJM_J). \quad (2)$$

The CSFs are anti-symmetrized many-electron functions built from products of one-electron Dirac orbitals and are eigenfunctions of the parity operator P, the total angular momentum operator J^2 and its projection on the z-axis J_z (Grant 2007; Froese Fischer et al. 2016). In the expression above, γ_i represents the configuration, coupling and other quantum numbers necessary to uniquely describe the CSFs.

The radial parts of the Dirac orbitals together with the mixing coefficients c_i are obtained in a self-consistent field (SCF) procedure. The set of SCF equations to be iteratively solved results from applying the variational principle on a weighted energy functional of all the studied states according to the extended optimal level (EOL) scheme (Dyall et al. 1989). The angular integrations needed for the construction of the energy functional are based on the second quantization method in the coupled tensorial form (Gaigalas et al. 1997, 2001).

The transverse photon (Breit) interaction, as well as the leading quantum electrodynamic (QED) corrections (vacuum polarization and self-energy) can be accounted for in subsequent relativistic configuration interaction (RCI) calculations (McKenzie et al. 1980). In the RCI calculations, the Dirac orbitals from the previous step are fixed and only the mixing coefficients of the CSFs are determined by diagonalizing the Hamiltonian matrix. All calculations were performed using the relativistic atomic structure package GRASP2K (Jönsson et al. 2013).

In the MCDHF relativistic calculations, the wave functions are expansions over jj-coupled CSFs. To identify the computed states and adapt the labeling conventions followed by the experimentalists, the ASFs are transformed from jj-coupling to a basis of $LS\,J$-coupled CSFs. In the GRASP2K code this is done using the methods developed by Gaigalas et al. (2003, 2004, 2017).

2.2. Transition parameters

Besides excitation energies, also lifetimes τ and transition parameters, such as emission transition rates A and weighted oscillator strengths gf, were computed. The transition parameters between two states $\gamma' P' J'$ and γPJ are expressed in terms of reduced matrix elements of the transition operator $\mathbf{T}$ (Grant 1974)

$$\langle \Psi(\gamma PJ) \| \mathbf{T} \| \Psi(\gamma' P' J') \rangle = \sum_{k,l} c_k c'_l \langle \Phi(\gamma_k PJ) \| \mathbf{T} \| \Phi(\gamma'_l P' J') \rangle. \quad (3)$$

For electric multipole transitions, there are two forms of the transition operator: the length, which in fully relativistic calculations is equivalent to the Babushkin gauge and the velocity form, equivalent to the Coulomb gauge. The transitions are governed by the outer part of the wave functions. The length form is more sensitive to this part of the wave functions and it is generally considered as the preferred form. Regardless, the agreement between the values of these two different forms can be used to indicate the accuracy of the wave functions (Froese Fischer 2009; Ekman et al. 2014). This is particularly useful when no experimental measurements are available. The transitions can be organized in groups, determined, for instance, by the magnitude of the transition rate value. A statistical analysis of the uncertainties of the transitions can then be performed. For each group of transitions, the average uncertainty to the length form of the computed transition rates is given by

$$\langle dT \rangle = \frac{1}{N} \sum_{i=1}^{N} \frac{|A_l^i - A_v^i|}{\max(A_l^i, A_v^i)}, \quad (4)$$

where A_l and A_v are respectively the transition rates in length and velocity form for a transition i and N is the number of the transitions belonging to a group. In this work, we only computed transition parameters for the electric dipole (E1) transitions. The electric quadrupole (E2) and magnetic multipole (Mk) transitions are much weaker and therefore less likely to be observed.

3. Calculations

3.1. Al I

In neutral aluminium, calculations were performed in the EOL scheme (Dyall et al. 1989) for 28 targeted states. These states belong to the $3s^2ns$ configurations with $n = 4, 5, 6$, the $3s^2nd$ configurations with $n = 3, ..., 6$, as well as the $3s3p^2$ and $3s^25g$ configurations, characterized by even parity and on the other hand, the $3s^2np$ configurations with $n = 3, .., 6$, as well as the $3s^24f$ and $3s^25f$ configurations, characterized by odd parity. These configurations define the so-called multireference (MR). From initial calculations and analysis of the eigenvector compositions, we deduced that all $3p^2nl$ configurations, in addition to the targeted $3s^2nl$, give considerable contributions to the total wave functions and should be included in the MR. Following the active set (AS) approach (Olsen et al. 1988; Sturesson et al. 2007), the CSF expansions (see eq. 2) were obtained by allowing single and restricted double (SD) substitutions of electrons from the reference (MR) orbitals to an AS of correlation orbitals. The AS is systematically increased by adding layers of orbitals to effectively build nearly complete wave functions. This is achieved by keeping track not only of the convergence of the computed excitation energies, but also of the other physical quantities of interest, such as the transition parameters here.

As a first step an MCDHF calculation was performed for the orbitals that are part of the MR. States with both even and odd parity were simultaneously optimized. Following this step, we continued to optimize six layers of correlation orbitals based on valence (VV) substitutions. The VV expansions were obtained by allowing SD substitutions from the three outer valence orbitals in the MR, with the restriction that there will be at most one substitution from orbitals with $n = 3$. In this manner, the correlation orbitals will occupy the space between the inner $n = 3$ valence orbitals and the outer orbitals involved in the higher Rydberg states (see Fig. 1). These orbitals have been shown to be of crucial importance for the transition probabilities, which are weighted towards this part of the space (Pehlivan Rhodin et al. 2017; Pehlivan Rhodin 2018). The six correlation layers correspond to the $12s, 12p, 12d, 11f, 11g$ and $10h$ set of orbitals.

Each MCDHF calculation was followed by an RCI calculation for an extended expansion, obtained by single, double and triple (SDT) substitutions from the valence orbitals. As a final step, an RCI calculation was performed for the largest SDT valence expansion augmented by a core-valence (CV) expansion. The CV expansion was obtained by allowing SD substitutions from the valence orbitals and the $2p^6$ core, with the restriction that there will be at most one substitution from $2p^6$. All the RCI calculations included the Breit interaction and the leading QED effects. Accounting for CV correlation does not lower the total

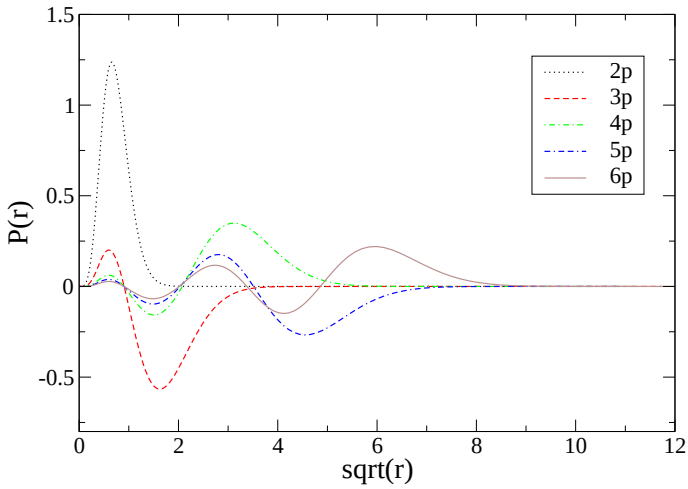

Fig. 1: The Al I Dirac-Fock radial orbitals for the p symmetry, as a function of $\sqrt{r}$. The $2p$ orbital is part of the core and the orbitals from $n = 3$ up to $n = 6$ are part of the valence electron cloud. We note that these orbitals occupy different regions in space and the overlap between some of the Rydberg states will be minor.

energies significantly, but it can have large effects on the energy separations and thus we considered it crucial. Core-valence correlation is also important for transition properties (Hibbert 1989). Core-core (CC) correlation, obtained by allowing double excitations from the core, is known to be less important and has not been considered in the present work. The number of CSFs in the final even and odd state expansions, accounting for both VV and CV electron correlation, were 4 362 628 and 2 889 385, respectively, distributed over the different J symmetries.

3.2. Al II

In the singly ionized aluminium, the calculations were more extended, including 78 targeted states. These states belong to the $3s^2$ ground configuration, as well as the $3p^2$, the $3sns$ configurations with $n = 4, ..., 7$, the $3snd$ with $n = 3, ..., 6$, the $3s5g$ and $3s6g$ configurations, characterized by even parity and on the other hand, the $3snp$ configurations with $n = 3, ..., 7$, the $3snf$ with $n = 4, 5, 6$, as well as the $3s6h$ and $3p3d$ configurations, characterized by odd parity. These configurations define the multireference (MR). In the computations of Al II, the EOL scheme was applied and the CSF expansions were obtained following the active set (AS) approach, accounting for VV and CV correlation. Al II is less complex and the CSF expansions generated from (SD) substitutions are not as large as the ones in Al I. Hence, we can afford both $2s$ and $2p$ orbitals to account for CV correlation. The $1s$ core orbital remained closed and as for Al I, core-core correlation was neglected. The MCDHF calculations were performed in a similar way as the calculations in Al I, yet no particular restrictions were imposed on the VV substitutions. We optimized six correlation layers corresponding to the $13s, 13p, 12d, 12f, 12g, 8h$ and $7i$ set of orbitals. Each MCDHF calculation was followed by an RCI calculation. At last, an RCI calculation was performed for the largest SD valence expansion augmented by the CV expansion. The number of CSFs in the final even and odd state expansions, accounting for both VV and CV electron correlation, were 911 795 and 1 269 797, respectively, distributed over the different J symmetries.

4. Results

4.1. Al I

In Table 1, the computed excitation energies, based on VV correlation, are given as a function of the increasing active set of orbitals. After adding the $n = 11$ correlation layer, we note that the energy values for all 28 targeted states have converged. For comparison, in the second last column the observed energies from the NIST Atomic Spectra Database (Kramida et al. 2018) are displayed. All energies but the ones belonging to the $3s3p^2$ configuration are already in good agreement with the NIST recommended values. The relative differences between theory and experiment for all three levels of the quartet $3s3p^2\ ^4P$ state is 3.1%, while the mean relative difference for the rest of the states is less than 0.2%. In the third last column, the computed excitation energies after accounting for CV correlation are displayed. When taking into account CV effects the agreement with the observed values is better overall. But most importantly, for the $3s3p^2\ ^4P$ levels the relative differences between observed and computed values decrease to less than 0.6%. The likelihood of the $1s^22s^22p^6$ core to overlap with the $3s3p^2$ cloud of electrons is much less relatively to the one for $3s^2nl$. Consequently, when CV correlation is taken into account the lowering of the $3s3p^2$ energy levels is much smaller than for levels belonging to any $3s^2nl$ configuration. Thus, the adjustments to the separation energies will be minor between the ground state $3s^23p$ and $3s^2nl$ levels, but significant between the $3s^23p$ and $3s3p^2$ levels. In the last column of Table 1, the differences $\Delta E = E_{\rm obs} - E_{\rm theor}$, between the final (CV) computed and the observed energies, are also displayed. In principle, there are two groups of values, with the one consisting of the $3s^2nd$ configurations exhibiting the smallest absolute discrepancies from the observed energies. For the rest, the absolute discrepancies are somewhat larger.

In the calculations, the labeling of the eigenstates is determined by the CSF with the largest coefficient in the expansion of eq. 2. When the same label is assigned to different eigenstates, a detailed analysis can be performed by displaying their LS-compositions. In Table 1, we note that two of the states have been assigned the same label, i.e. $3s^24d\ ^2D$, and thus the subscripts a and b are used to distinguish them. In Table 2, we give the LS-composition of all computed $3s^2nd\ ^2D$ states, including the three most dominant CSFs. The $3s^24d\ ^2D$ term appears twice as the CSF with the largest LS-composition. Moreover, the admixture of the $3s3p^2\ ^2D$ in the lowest four $3s^2nd\ ^2D$ states is rather strong and adds up to 65%. That being so, the $3s3p^2\ ^2D$ does not exist in the calculated spectrum as a localized state. For comparison, in the last column of Table 2, the labeling of the observed $3s^2nd\ ^2D$ states is also given. In the observed configurations presented by NIST (Kramida et al. 2018), the second highest $3s^2nd\ ^2D$ term has not been given any specific label and it is therefore designated as $y\ ^2D$. The higher ^2D terms are designated as $3s^24d$, $3s^25d$ and so on.

In Table 3, the current results for the lowest excitation energies are compared with the ones from the MCHF-BP calculations by Froese Fischer et al. (2006). The latter calculations are extended up to levels corresponding to the doublet $3s^24p\ ^2P$ state. The differences ΔE between observed and computed energies are given in the last two columns for the different computational approaches. As seen, when using the current MCDHF and RCI method, the agreement with the observed energies is substantially improved for all levels and in particular, for the ones belonging to the quartet $3s3p^2\ ^4P$ state. In the MCHF-BP calculations, core-valence correlation was neglected. As mentioned above and also acknowledged by Froese Fischer et al. (2006),

Table 1: Computed excitation energies in cm^{-1} for the 28 lowest states in Al I. The energies are given as a function of the increasing active set of orbitals, accounting for VV correlation, where n indicates the maximum principle quantum number of the orbitals included in the active set. In the third last column, the final energy values are displayed after accounting for CV correlation. The differences ΔE between the final computations and the observed values are shown in the last column. The sequence and labeling of the configurations and $LS\,J$-levels are in accordance with the final (CV) computed energies. The $3s^2 4d\ ^2D$ term is assigned twice throughout the calculations (see also Table 2) and the subscripts a and b are being used to distinguish them. See text for more details.

			VV								
Pos.	Conf.	$LS\,J$	$n = 7$	$n = 8$	$n = 9$	$n = 10$	$n = 11$	$n = 12$	CV	E_{obs} [(1)]	ΔE
1	$3s^2\,3p$	$^2P^o_{1/2}$	0	0	0	0	0	0	0	0	0
2		$^2P^o_{3/2}$	108	108	108	108	108	108	104	112	8
3	$3s^2\,4s$	$^2S_{1/2}$	25 318	25 377	25 416	25 419	25 427	25 429	25 196	25 348	152
4	$3s\,3p^2$	$^4P_{1/2}$	27 788	27 966	28 073	28 085	28 109	28 111	28 863	29 020	157
5		$^4P_{3/2}$	27 833	28 011	28 118	28 130	28 154	28 156	28 907	29 067	160
6		$^4P_{5/2}$	27 906	28 085	28 191	28 204	28 227	28 230	28 981	29 143	162
7	$3s^2\,3d$	$^2D_{3/2}$	32 211	32 077	32 135	32 139	32 150	32 150	32 414	32 435	21
8		$^2D_{5/2}$	32 212	32 079	32 137	32 141	32 152	32 152	32 416	32 437	21
9	$3s^2\,4p$	$^2P^o_{1/2}$	32 770	32 879	32 935	32 937	32 946	32 949	32 801	32 950	149
10		$^2P^o_{3/2}$	32 786	32 894	32 951	32 952	32 962	32 964	32 814	32 966	152
11	$3s^2\,5s$	$^2S_{1/2}$	37 493	37 637	37 693	37 694	37 704	37 706	37 512	37 689	177
12	$3s^2\,4d$	$^2D_{3/2\ a}$	38 733	38 659	38 711	38 707	38 717	38 718	38 951	38 929	-22
13		$^2D_{5/2\ a}$	38 736	38 664	38 717	38 712	38 722	38 724	38 957	38 934	-23
14	$3s^2\,5p$	$^2P^o_{1/2}$	40 038	40 187	40 252	40 249	40 259	40 262	40 101	40 272	171
15		$^2P^o_{3/2}$	40 043	40 193	40 258	40 255	40 265	40 268	40 106	40 278	172
16	$3s^2\,4f$	$^2F^o_{5/2}$	41 050	41 209	41 282	41 287	41 297	41 300	41 163	41 319	156
17		$^2F^o_{7/2}$	41 050	41 209	41 282	41 287	41 297	41 300	41 163	41 319	156
18	$3s^2\,6s$	$^2S_{1/2}$	41 897	42 069	42 133	42 135	42 144	42 143	41 964	42 144	180
19	$3s^2\,4d$	$^2D_{3/2\ b}$	42 105	42 071	42 121	42 108	42 119	42 121	42 232	42 234	2
20		$^2D_{5/2\ b}$	42 109	42 075	42 126	42 112	42 123	42 125	42 237	42 238	1
21	$3s^2\,6p$	$^2P^o_{1/2}$	43 076	43 246	43 316	43 311	43 321	43 324	43 160	43 335	175
22		$^2P^o_{3/2}$	43 079	43 249	43 318	43 313	43 324	43 326	43 162	43 338	176
23	$3s^2\,5f$	$^2F^o_{5/2}$	43 549	43 721	43 795	43 801	43 811	43 813	43 660	43 831	171
24		$^2F^o_{7/2}$	43 549	43 721	43 795	43 801	43 811	43 813	43 660	43 831	171
25	$3s^2\,5g$	$^2G_{7/2}$	43 576	43 763	43 838	43 845	43 856	43 859	43 687	43 876	189
26		$^2G_{9/2}$	43 576	43 763	43 838	43 845	43 856	43 859	43 687	43 876	189
27	$3s^2\,5d$	$^2D_{3/2}$	44 034	44 059	44 115	44 096	44 106	44 109	44 126	44 166	40
28		$^2D_{5/2}$	44 036	44 062	44 117	44 099	44 109	44 111	44 129	44 169	40

References. [(1)]NIST Atomic Spectra Database 2018 (Kramida et al. 2018).

Table 2: LS-composition of the computed states belonging to the strongly mixed $3s^2nd$ Rydberg series in Al I. The three most dominant LS-components are displayed. The first percentage value corresponds to the assigned configuration and term. In all these cases, the percentages for the two different $LS\,J$-levels are the same and therefore given in the same line. In the last column, we provide the labeling of the corresponding observed terms as given in the NIST Database. The first column refers to the positions according to Table 1.

Pos.	Conf.	$LS\,J$	LS-composition	Label used in NIST
7,8	$3s^2\,3d$	$^2D_{3/2,5/2}$	$0.67 + 0.19\ 3s\,3p^2\ ^2D + 0.04\ 3s^2\,4d\ ^2D$	$3s^2\,3d\ \ ^2D_{3/2,5/2}$
12,13	$3s^2\,4d$	$^2D_{3/2,5/2\ a}$	$0.41 + 0.22\ 3s^2\,3d\ ^2D + 0.21\ 3s\,3p^2\ ^2D$	$3s^2\,nd\ \ y\ ^2D_{3/2,5/2}$
19,20	$3s^2\,4d$	$^2D_{3/2,5/2\ b}$	$0.44 + 0.25\ 3s^2\,5d\ ^2D + 0.15\ 3s\,3p^2\ ^2D$	$3s^2\,4d\ \ ^2D_{3/2,5/2}$
27,28	$3s^2\,5d$	$^2D_{3/2,5/2}$	$0.58 + 0.19\ 3s^2\,6d\ ^2D + 0.10\ 3s\,3p^2\ ^2D$	$3s^2\,5d\ \ ^2D_{3/2,5/2}$

References. [(1)]Kramida et al. (2018).

capturing such correlation effects is crucial for 3s-hole states, such as states with significant $3s3p^2$ composition. Furthermore, the $\Delta E_{\text{MCHF-BP}}$ values do not always have the same sign, while the ΔE_{RCI} differences are consistently positive. This is particularly important when calculating transition properties. On average, properties for transitions between two levels for which the differences $\Delta E_{\text{MCHF-BP}}$ have opposite sign will be estimated less accurately.

The complete transition data, for all computed E1 transitions in Al I, can be found in Table 10. In Table 10, the transition energies, wavelengths and the length form of the transition rates A and weighted oscillator strengths gf are given. Based on the

Table 3: Observed and computed excitation energies in cm^{-1} for the 10 and 20 lowest states in Al I and Al II, respectively. In the last two columns, the difference ΔE between observed and computed energies is compared for the current RCI and previous MCHF-BP calculations.

Pos.	Conf.	$LS\,J$	E_{obs} [(1)]	E_{RCI} [(2)]	ΔE_{RCI} [(2)]	$\Delta E_{MCHF\text{-}BP}$ [(3)]
			Al I			
1	$3s^2\,3p$	$^2P^o_{1/2}$	0	0	0	0
2		$^2P^o_{3/2}$	112	104	8	22
3	$3s^2\,4s$	$^2S_{1/2}$	25 348	25 196	152	-235
4	$3s\,3p^2$	$^4P_{1/2}$	29 020	28 863	157	940
5		$^4P_{3/2}$	29 067	28 907	160	949
6		$^4P_{5/2}$	29 143	28 981	162	964
7	$3s^2\,3d$	$^2D_{3/2}$	32 435	32 414	21	250
8		$^2D_{5/2}$	32 437	32 416	21	251
9	$3s^2\,4p$	$^2P^o_{1/2}$	32 950	32 801	149	-98
10		$^2P^o_{3/2}$	32 966	32 814	152	-94
			Al II			
1	$3s^2$	$^1S_0$	0	0	0	0
2	$3s\,3p$	$^3P^o_0$	37 393	37 445	-52	9
3		$^3P^o_1$	37 454	37 503	-49	8
4		$^3P^o_2$	37 578	37 626	-48	6
5		$^1P^o_1$	59 852	59 982	-130	-177
6	$3p^2$	$^1D_2$	85 481	85 692	-211	-305
7	$3s\,4s$	$^3S_1$	91 275	91 425	-150	-376
8	$3p^2$	$^3P_0$	94 085	94 211	-126	-107
9		$^3P_1$	94 147	94 264	-117	-111
10		$^3P_2$	94 269	94 375	-106	-113
11	$3s\,4s$	$^1S_0$	95 351	95 543	-192	-400
12	$3s\,3d$	$^3D_2$	95 549	95 791	-242	-527
13		$^3D_1$	95 551	95 794	-243	-527
14		$^3D_3$	95 551	95 804	-253	-529
15	$3s\,4p$	$^3P^o_0$	105 428	105 582	-154	-357
16		$^3P^o_1$	105 442	105 594	-152	-360
17		$^3P^o_2$	105 471	105 623	-152	-363
18		$^1P^o_1$	106 921	107 132	-211	-365
19	$3s\,3d$	$^1D_2$	110 090	110 330	-240	-475
20	$3p^2$	$^1S_0$	111 637	112 086	-449	-445

References. [(1)]Kramida et al. (2018); [(2)]present calculations; [(3)]Froese Fischer et al. (2006).

agreement between the length and velocity forms of the computed transition rates A_{RCI}, a statistical analysis of the uncertainties can be preformed. The transitions were arranged in four groups based on the magnitude of the A_{RCI} values. The first two groups contain all the weak transitions with transition rates up to $A = 10^6$ s^{-1}, while the next two groups contain the strong transitions with $A > 10^6$ s^{-1}. In Table 4, the average value of the uncertainties $\langle dT \rangle$ (see eq. 4) is given for each group of transitions. To better understand how the individual uncertainties dT are distributed, the maximum value, as well as the value Q_3 containing 75% of the lowest computed dT values (third quartile) are also given in Table 4. When examining the predicted uncertainties of the individual groups, we deduce that for all the strong transitions dT always remains below 15%. In fact, the majority of the strong transitions is associated with uncertainties of the order of a few per cent, which justifies the low average values. Contrary to the strong transitions, the weaker transitions are associated with considerably larger uncertainties. This is even more pronounced for the first group of transitions, where A is less than 10^5 s^{-1}. The weak E1 transitions are challenging, and therefore interesting, from a theoretical point of view, yet they are less likely to be observed. The computation of transition properties in the system of Al I is overall far from trivial due to the extreme mixing of the $3s^2nd\ ^2D$ series. Transitions involving any ^2D state as upper or lower level appear to be associated with large uncertainties. However, the predicted energy separations are in excellent agreement with observations, meaning that the LS-composition of the $3s^2nd\ ^2D$ states is well described. This fact should serve as a quality indicator of the computed transition data.

Transition rates A_{obs} evaluated from experimental measurements are, in Table 5, compared with the current RCI theoretical values, as well as values from the MCHF-BP calculations by Froese Fischer et al. (2006) and the close coupling (CC) calculations by Mendoza et al. (1995). Despite the fact that the measurements by Davidson et al. (1990) are more recent compared to the compiled values by Wiese and Martin (1980), the latter seem to be in better overall agreement with the transition rates predicted by the RCI calculations. In all cases, the A_{RCI} values fall into the range of the estimated uncertainties by Wiese and Martin (1980). The only exceptions are the transitions with $3s^24d\ ^2D_{3/2,5/2\ a}$ as upper levels, for which the A_{RCI} values agree better with the ones suggested by Davidson et al. (1990). Although the evaluated transition rates by Vujnović et al. (2002) slightly differ from the other observations, they are still in fairly good agreement with the present work. For the $3s^24p\ ^2P^o_{3/2} \rightarrow 3s^24s\ ^2S_{1/2}$ and $3s^23d\ ^2D_{5/2} \rightarrow 3s^23p^2P^o_{3/2}$

Table 4: Statistical analysis of the uncertainties of the computed transition rates in Al I and Al II. The transition rates are arranged in four groups and in the forth column, the number of transitions belonging to each group is given. In the last three columns, the average value, the value Q_3 containing 75% of the lowest computed dT values, as well as the maximum value are given for each group of transitions. All transition rates are given in s^{-1}.

	$A_{\rm RCI}^{\rm low}$	$A_{\rm RCI}^{\rm high}$	No.Trans.	$\langle dT \rangle$	Q_3	max
			Al I			
1		1.00E+05	31	0.62	0.83	0.98
2	1.00E+05	1.00E+06	25	0.29	0.37	0.81
3	1.00E+06	1.00E+07	24	0.055	0.076	0.15
4	1.00E+07		20	0.043	0.073	0.14
			Al II			
1		1.00E+05	109	0.07	0.11	0.61
2	1.00E+05	1.00E+06	81	0.09	0.11	0.67
3	1.00E+06	1.00E+07	99	0.043	0.036	0.39
4	1.00E+07		141	0.011	0.009	0.12

transitions, the values by Vujnović et al. (2002) are better reproduced by the $A_{\rm MCHF\text{-}BP}$ results, yet not enough correlation is included in the calculations by Froese Fischer et al. (2006) and the transition rates predicted by the RCI calculations should be considered as more accurate. Whenever values from the close coupling (CC) calculations are presented to complement the MCHF-BP results, the $A_{\rm RCI}$ values appear to be in better agreement with the experimental values. Exceptionally, for the $3s^25d\ ^2D_{3/2,5/2} \rightarrow 3s^23p\ ^2P^o_{3/2}$ transitions, the $A_{\rm CC}$ values by Mendoza et al. (1995) approach more the corresponding experimental values. Even so, the $A_{\rm RCI}$ values are still within the given experimental uncertainties. One should bear in mind that according to the estimation of uncertainties by Kelleher and Podobedova (2008b) the $A_{\rm CC}$ values carry relative uncertainties up to 30%. On the contrary, based on the agreement between length and velocity forms, the estimated uncertainties of the current RCI calculations for the above mentioned transitions are of the order of a few percent. Therefore, we suggest that the current transition rates are used as a reference.

From the computed E1 transition rates, the lifetimes of the excited states are estimated. Transition data for other transitions than E1 have not been computed in this work, since the contributions to the lifetimes from magnetic or higher electric multipoles are expected to be negligible. In Table 6, the currently computed lifetimes are given in both length τ_l and velocity τ_v forms. The agreement between these two forms probes the level of accuracy of the calculations. Because of the poor agreement between the length and velocity form of the quartet $3s3p^2\ ^4P$ and doublet $3s^26p\ ^2P$ states, the average relative difference appears overall to be $\sim$ 8%. The differences between the length and velocity gauges of the quartet $3s3p^2\ ^4P$ states are of the order of 25% in average. These long-lived states are associated with weak transitions and computations involving such transitions are, as mentioned before, rather challenging. In addition, we note that the relative differences corresponding to the $3s^26p\ ^2P$ states exceed 40%. As the computations involve Rydberg series, states between the lowest and highest computed levels might not occupy the same region in space. Nevertheless, these states are part of the same multireference (MR). The highest computed levels correspond to configurations with orbitals up to $n = 6$, such as $3s^26p$. To obtain a better description of those levels it is probably necessary to perform initial calculations including in the MR $3s^2nl$ configurations with $n = 7$ and maybe even $n = 8$. This would lead to a more complete and balanced orbital set (Pehlivan Rhodin et al. 2017). When excluding the above mentioned states, the mean relative difference between τ_l and τ_v is $\sim$ 3%, which is satisfactory.

In Table 6, the lifetimes from the current RCI calculations are also compared with results from the MCHF-BP calculations by Froese Fischer et al. (2006) and observations. Only for the $3s^24p\ ^2P$ state, separated observed values of the lifetimes are given for the two fine-structure components. For the rest of the measured lifetimes, a single value for the two fine-structure levels is provided. As seen, the overall agreement between the theoretical and the measured lifetimes $\tau_{\rm obs}$ is rather good. However, the measured lifetimes are better represented by the current RCI results compared to the MCHF-BP ones. For most of the states, the differences between the RCI and MCHF-BP values are small, except for the levels of the quartet $3s3p^2\ ^4P$ state. For these long-lived states, no experimental lifetimes exist for comparison.

4.2. Al II

In Table 8, the computed excitation energies, based on VV correlation, are given as a function of the increasing active set of orbitals. When adding the $n = 12$ correlation layer, the values for all computed energy separations have converged. The agreement with the NIST (Kramida et al. 2018) observed energies is, at this point, fairly good. The mean relative difference between theory and experiment is of the order of 1.2%. However, when accounting for CV correlation the agreement with the observed values is significantly improved, resulting in a mean relative difference being less than 0.2%. Accounting for CV effects also results in a labeling of the eigenstates that matches with observations. For instance, when only VV correlation is taken into account, the ^3F triplet with the highest energy is labeled as a $3s6f$ level. After taking CV effects into account, the eigenstates of this triplet are assigned the $3p3d$ configuration being now the one with the largest expansion coefficient, which agree with observations. There are no experimental excitation energies for the singlet and triplet $3s6h\ ^{1,3}H$ terms. In the last column of Table 8, the differences ΔE, between computed and observed energies, are displayed. All ΔE values maintain the same sign, being negative.

In Table 3, a comparison between the present computed excitation energies and the ones from the MCHF-BP calculations by Froese Fischer et al. (2006) is also performed for Al II. The latter spectrum calculations are extended up to levels correspond-

Table 5: Comparison between computed and observed transition rates A in s^{-1}, for selected transitions in Al I. The present values from the RCI calculations are given in the third column. In the next two columns, theoretical values from former MCHF-BP and close coupling (CC) calculations are displayed. The CC values complement the MCHF-BP ones, which are restricted to transitions between levels in the lower part of the Al I spectrum. The last two columns contain the results from experimental observations. The experimental results go along with a letter-grade, whenever accessible, which indicates their accuracy level.

Upper	Lower	$A_{\rm RCI}$ [2]	$A_{\rm MCHF\text{-}BP}$ [3]	$A_{\rm CC}$ [4a]	$A_{\rm obs}$ [5],[6],[7]	$A_{\rm obs}$ [8]
$3s^2\,4s\ ^2S_{1/2}$	$3s^2\,3p\ ^2P^o_{1/2}$	4.966E+07	5.098E+07		4.93E+07 [5] C	4.70E+07 B
	$3s^2\,3p\ ^2P^o_{3/2}$	9.884E+07	10.15E+07		9.80E+07 [5] C	9.90E+07 B
$3s^2\,5s\ ^2S_{1/2}$	$3s^2\,3p\ ^2P^o_{1/2}$	1.277E+07			1.33E+07 [5] C	1.42E+07 C+
	$3s^2\,3p\ ^2P^o_{3/2}$	2.534E+07			2.64E+07 [5] C	2.84E+07 C+
$3s^2\,5s\ ^2S_{1/2}$	$3s^2\,4p\ ^2P^o_{1/2}$	3.815E+06				3.00E+06 D
	$3s^2\,4p\ ^2P^o_{3/2}$	7.599E+06				6.00E+06 D
$3s^2\,4p\ ^2P^o_{1/2}$	$3s^2\,4s\ ^2S_{1/2}$	1.580E+07	1.507E+07		1.69E+07 [6] C+	1.60E+07 A
$3s^2\,4p\ ^2P^o_{3/2}$	$3s^2\,4s\ ^2S_{1/2}$	1.587E+07	1.514E+07		1.69E+07 [6] C+	1.50E+07 B
$3s^2\,3d\ ^2D_{3/2}$	$3s^2\,3p\ ^2P^o_{1/2}$	6.542E+07	5.651E+07		6.30E+07 [5] C	5.90E+07 C+
	$3s^2\,3p\ ^2P^o_{3/2}$	1.321E+07	1.140E+07			(1.20)E+07
$3s^2\,3d\ ^2D_{5/2}$	$3s^2\,3p\ ^2P^o_{3/2}$	7.877E+07	6.806E+07		7.40E+07 [5] C	7.10E+07 A
$3s^2\,4d\ ^2D_{3/2\ a}$	$3s^2\,3p\ ^2P^o_{1/2}$	1.722E+07			1.92E+07 [7] C+	
					2.30E+07 [5] C	
	$3s^2\,3p\ ^2P^o_{3/2}$	3.293E+06		5.99E+06	3.80E+06 [7] C+	
					4.40E+06 [5] C	
$3s^2\,4d\ ^2D_{5/2\ a}$	$3s^2\,3p\ ^2P^o_{3/2}$	2.010E+07		3.60E+07	2.30E+07 [7]	
					2.80E+07 [5] C	
$3s^2\,4d\ ^2D_{3/2\ b}$	$3s^2\,3p\ ^2P^o_{1/2}$	7.128E+07		7.61E+07	7.20E+07 [5] C	
					5.26E+07 [7]	
	$3s^2\,3p\ ^2P^o_{3/2}$	1.386E+07		1.51E+07	1.40E+07 [5] C	
					1.05E+07 [7] A	
$3s^2\,4d\ ^2D_{5/2\ b}$	$3s^2\,3p\ ^2P^o_{3/2}$	8.412E+07		9.07E+07	8.60E+07 [5] C	
					6.31E+07 [7]	
$3s^2\,5d\ ^2D_{3/2}$	$3s^2\,3p\ ^2P^o_{1/2}$	8.204E+07			6.60E+07 [5] C	
					5.76E+07 [7]	
	$3s^2\,3p\ ^2P^o_{3/2}$	1.596E+07		1.26E+07	1.30E+07 [5] C	
					1.15E+07 [7]	
$3s^2\,5d\ ^2D_{5/2}$	$3s^2\,3p\ ^2P^o_{3/2}$	9.706E+07		7.58E+07	7.90E+07 [5] C	
					6.91E+07 [7]	

Notes. All theoretical transition rates are presented in length form. The correspondance between the accuracy ratings and the estimated relative uncertainty of the experimental results is: $A :\leq 3\%$, $B :\leq 10\%$, $C+ :\leq 15\%$, $C :\leq 25\%$, $D+ :\leq 30\%$, $D :\leq 50\%$

References. [2]Present calculations; [3]Froese Fischer et al. (2006); [4a]Mendoza et al. (1995); [5]Wiese and Martin (1980); [6]Buurman et al. (1986); [7]Davidson et al. (1990); [8]Vujnović et al. (2002).

ing to the singlet $3p^2\ ^1S$ state and all types of correlation, i.e. VV, CV and CC, were accounted for. Both computational approaches are highly accurate, yet the majority of the levels is better represented by the current RCI results. The average relative difference for the RCI values is $\sim 0.2\%$ and for the MCHF-BP $\sim 0.3\%$. Moreover, the $\Delta E_{\rm MCHF\text{-}BP}$ values do not always maintain the same sign, while the $\Delta E_{\rm RCI}$ values do. Hence, in general, the MCHF-BP calculations do not predict the transition energies and properties as precisely as the present RCI method.

For all computed E1 transitions in Al II, the transition data can be found in Table 11. In Table 4, a statistical analysis of the uncertainties to the computed transition rates $A_{\rm RCI}$ is performed in a similar way as done for Al I. The transitions are also arranged here in four groups. Following the conclusions by Pehlivan Rhodin et al. (2017) and Pehlivan Rhodin (2018), the transitions involving any of the $3s7p\ ^{1,3}P$ states have been excluded from this analysis. The discrepancies between the length and velocity forms for transitions including the $3s7p\ ^{1,3}P$ states are consistently large and thus the computed transition rates are not trustworthy. We note that overall, the average uncertainty, as well as the value that includes 75% of the data appear to be smaller, for each group of transitions, compared to the predicted ones in Al I. Nevertheless, the maximum values of the uncertainties for the last two groups are larger in comparison to Al I. This is due to some transitions involving $3p3d\ ^3F$ as upper level. The strong mixing between the $3p3d\ ^3F$ and the $3s6f\ ^3F$ levels results in strong cancellation effects. Such effects often hamper the accuracy of the computed transition data and result in large discrepancies between the length and velocity forms.

In Table 7, current RCI theoretical transition rates are compared with the values from the MCHF-BP calculations by Froese Fischer et al. (2006) and, whenever available, results from the B-spline configuration interaction (BSCI) calculations by Chang and Fang (1995). For the majority of the transitions, there is an excellent agreement between the RCI and MCHF-BP values with the relative difference being less than 1%. Some of the largest discrepancies are observed for the $\{3s3d, 3p^2\}\ ^1D \rightarrow 3s3p\ ^{\{1,3\}}P^o$ transitions. According to Froese Fischer et al. (2006), correlation is extremely important for transitions from such ^1D states. In the MCHF-BP calcula-

Table 6: Comparison between computed and observed lifetimes τ in seconds, for the 26 lowest excited states in Al I. For the current RCI calculations both length τ_l and velocity τ_v forms are displayed. In the second last column, the predicted lifetimes from MCHF-BP calculations are given in length form. The last column contains available lifetimes from experimental measurements, together with their uncertainties.

			RCI [2]		MCHF-BP [3]	Expt.[6],[7],[9]
Pos.	Conf.	LSJ	τ_l	τ_v	τ_l	$\tau_{\rm obs}$
1	$3s^2\,4s$	$^2S_{1/2}$	6.734E-09	6.745E-09	6.558E-09	6.85(6)E-09 [6]
2	$3s\,3p^2$	$^4P_{1/2}$	1.652E-03	1.182E-03	4.950E-03	
3		$^4P_{3/2}$	6.702E-03	6.911E-03	13.24E-03	
4		$^4P_{5/2}$	2.604E-03	3.681E-03	9.486E-03	
5	$3s^2\,3d$	$^2D_{3/2}$	1.272E-08	1.372E-08	1.472E-08	1.40(2)E-08 [6]
6		$^2D_{5/2}$	1.270E-08	1.371E-08	1.469E-08	1.40(2)E-08 [6]
7	$3s^2\,4p$	$^2P^o_{1/2}$	6.329E-08	6.357E-08	6.621E-08	6.05(9)E-08 [9]
8		$^2P^o_{3/2}$	6.300E-08	6.328E-08	6.590E-08	6.5 (2) E-08 [9]
9	$3s^2\,5s$	$^2S_{1/2}$	2.019E-08	2.027E-08		1.98(5)E-08 [6]
10	$3s^2\,4d$	$^2D_{3/2\,a}$	3.117E-08	2.919E-08		2.95(7)E-08 [6]
11		$^2D_{5/2\,a}$	3.158E-08	2.953E-08		2.95(7)E-08 [6]
12	$3s^2\,5p$	$^2P^o_{1/2}$	2.448E-07	2.532E-07		2.75(8)E-07 [6]
13		$^2P^o_{3/2}$	2.429E-07	2.512E-07		2.75(8)E-07 [6]
14	$3s^2\,4f$	$^2F^o_{5/2}$	6.041E-08	6.162E-08		
15		$^2F^o_{7/2}$	6.041E-08	6.160E-08		
16	$3s^2\,6s$	$^2S_{1/2}$	4.812E-08	4.885E-08		
17	$3s^2\,4d$	$^2D_{3/2\,b}$	1.136E-08	1.083E-08		1.32(3)E-08 [7]
18		$^2D_{5/2\,b}$	1.150E-08	1.093E-08		1.32(3)E-08 [7]
19	$3s^2\,6p$	$^2P^o_{1/2}$	4.886E-07	6.952E-07		
20		$^2P^o_{3/2}$	4.845E-07	6.882E-07		
21	$3s^2\,5f$	$^2F^o_{7/2}$	1.176E-07	1.172E-07		
22		$^2F^o_{5/2}$	1.175E-07	1.172E-07		
23	$3s^2\,5g$	$^2G_{7/2}$	2.301E-07	2.315E-07		
24		$^2G_{9/2}$	2.301E-07	2.315E-07		
25	$3s^2\,5d$	$^2D_{3/2}$	1.011E-08	9.855E-09		14.0(2)E-09 [7]
26		$^2D_{5/2}$	1.020E-08	9.921E-09		14.0(2)E-09 [7]

References. [2]Present calculations; [3]Froese Fischer et al. (2006); [6]Buurman et al. (1986); [7]Davidson et al. (1990); [9]Buurman and Dönszelmann (1990).

tions, all three types of correlation, i.e. VV, CV and CC, have been accounted for, however the CSF expansions obtained from SD-substitutions are not as large as in the present calculations and the LS-composition of the configurations might not be predicted as accurately. Hence, the evaluation of line strengths for transitions involving ^1D states and in turn the computation of transition rates involving these states will be affected. Computed transition rates using the BSCI approach are provided for transitions that involve only singlet states. The BSCI calculations do not account for the relativistic interaction and no separate values are given for the different fine-structure components of triplet states. For the $3p^2\ ^1D \rightarrow 3s3p\ ^1P^o$ transition, the discrepancy between the RCI and BSCI values is also quite large. On the other hand, for the $3s3d\ ^1D \rightarrow 3s3p\ ^1P^o$ transition, the BSCI result is in perfect agreement with the present $A_{\rm RCI}$ value. The agreement between the current RCI and BSCI transition rates exhibits a broad variation. The advantage of the BSCI approach is that it takes into account the effect of the positive-energy continuum orbitals in an explicit manner. Nevertheless, the parametrized model potential that is being used in the work by Chang and Fang (1995) is not sufficient to describe states that are strongly mixed. At last, we note the discrepancy for the $3s4p\ ^1P^o \rightarrow 3s^2\ ^1S_0$ transition, which is quite large between the RCI and MCHF-BP values and inexplicably large between the RCI and BSCI ones.

In the singly ionized aluminium, measurements of transition properties are available only for a few transitions. In Table 7, the available experimental results are compared with the theoretical results from the current RCI calculations, as well as the former calculations by Froese Fischer et al. (2006) and Chang and Fang (1995). Transition rates have been experimentally observed for the $3s3p\ ^{1,3}P^o_1 \rightarrow 3s^2\ ^1S_0$ transitions in the works by Kernahan et al. (1979); Smith (1970); Berry et al. (1970); Head et al. (1976) and Träbert et al. (1999); Johnson et al. (1986), respectively. In Table 7, the average value of these works is displayed. The agreement with the current RCI results is fairly good. Nonetheless, the averaged $A_{\rm obs}$ by Träbert et al. (1999) and Johnson et al. (1986) is in better agreement with the value by Froese Fischer et al. (2006). Additionally, Vujnović et al. (2002) provided experimental transition rates for the $3p^2\ ^1D_2 \rightarrow 3s3p\ ^1P_1$ and $3p^2\ ^1D_2 \rightarrow 3s3p\ ^3P_{1,2}$ transitions by measuring relative intensities of spectral lines. These experimental results, however, differ from the theoretical values.

In the last portion of Table 7, current transition rates for transitions between states with higher energies are compared with the results from the close coupling (CC) calculations by Butler et al. (1993) and the early results from the configuration interaction (CI) calculations by Chang and Wang (1987). The results from the latter two calculations are found to be in very good agreement. Furthermore, the agreement between the RCI results

Table 7: Comparison between computed and observed transition rates A in s^{-1}, for selected transitions in Al II. The present values from the RCI calculations are given in the third column. In the next two columns, theoretical values from former MCHF-BP, close coupling (CC), configuration interaction (CI) and B-spline configuration interaction (BSCI) calculations are displayed. The last column contains the results from experimental observations. All theoretical transition rates are presented in length form.

Upper	Lower	$A_{\rm RCI}$ [2]	$A_{\rm theor}$ [3],[4b]	$A_{\rm theor}$ [10],[11]	$A_{\rm obs}$ [8]
$3s3p\ ^3P^o_1$	$3s^2\ ^1S_0$	3.054E+03	3.277E+03 [3]		3.30E+03 [13]
$3s3p\ ^1P^o_1$	$3s^2\ ^1S_0$	1.404E+09	1.400E+09 [3]	1.486E+09 [11]	1.45E+09 [12]
$3s4s\ ^3S_1$	$3s3p\ ^3P^o_0$	8.612E+07	8.572E+07 [3]		
	$3s3p\ ^3P^o_1$	2.555E+08	2.547E+08 [3]		
	$3s3p\ ^3P^o_2$	4.173E+08	4.162E+08 [3]		
$3s4s\ ^1S_0$	$3s3p\ ^1P^o_1$	3.422E+08	3.455E+08 [3]	3.408E+08 [11]	
$3p^2\ ^1D_2$	$3s3p\ ^1P^o_1$	2.523E+05	3.804E+05 [3]	3.980E+05 [11]	1.84E+04 [8]
	$3s3p\ ^3P^o_1$	1.790E+04	2.016E+04 [3]		0.19E+04 [8]
	$3s3p\ ^3P^o_2$	2.827E+04	3.141E+04 [3]		0.30E+04 [8]
$3p^2\ ^3P_0$	$3s3p\ ^3P^o_1$	1.236E+09	1.235E+09 [3]		
$3p^2\ ^3P_1$	$3s3p\ ^3P^o_0$	4.148E+08	4.144E+08 [3]		
	$3s3p\ ^3P^o_1$	3.058E+08	3.062E+08 [3]		
	$3s3p\ ^3P^o_2$	5.170E+08	5.167E+08 [3]		
$3p^2\ ^3P_2$	$3s3p\ ^3P^o_1$	3.145E+08	3.144E+08 [3]		
	$3s3p\ ^3P^o_2$	9.264E+08	9.272E+08 [3]		
$3p^2\ ^1S_0$	$3s3p\ ^1P^o_1$	1.020E+09	6.738E+08 [3]		
	$3s3p\ ^3P^o_1$	5.021E+08	3.399E+07 [3]		
$3s3d\ ^3D_2$	$3s3p\ ^3P^o_1$	8.977E+08	9.072E+08 [3]		
	$3s3p\ ^3P^o_2$	3.019E+08	3.046E+08 [3]		
$3s3d\ ^3D_3$	$3s3p\ ^3P^o_2$	1.197E+09	1.208E+09 [3]		
$3s3d\ ^1D_2$	$3s3p\ ^1P^o_1$	1.388E+09	1.429E+09 [3]	1.388E+09 [11]	
$3s4p\ ^3P^o_0$	$3s4s\ ^3S_1$	5.639E+07	5.705E+07 [3]		
	$3s3d\ ^3D_1$	1.556E+07	1.520E+07 [3]		
$3s4p\ ^3P^o_1$	$3s4s\ ^3S_1$	5.649E+07	5.724E+07 [3]		
	$3s3d\ ^3D_1$	3.905E+06	3.816E+06 [3]		
	$3s3d\ ^3D_2$	1.172E+07	1.146E+07 [3]		
$3s4p\ ^3P^o_2$	$3s4s\ ^3S_1$	5.683E+07	5.762E+07 [3]		
	$3s3d\ ^3D_1$	1.568E+05	1.541E+05 [3]		
	$3s3d\ ^3D_2$	2.361E+06	2.312E+06 [3]		
	$3s3d\ ^3D_3$	1.319E+07	1.294E+07 [3]		
$3s4p\ ^1P^o_1$	$3s^2\ ^1S_0$	1.527E+06	0.981E+06 [3]	5.079E+06 [11]	
	$3p^2\ ^1D_2$	5.835E+07	5.897E+07 [3]	6.307E+07 [11]	
	$3s4s\ ^1S_0$	3.109E+07	2.965E+07 [3]	3.111E+07 [11]	
$3p3d\ ^3F^o_2$	$3s3d\ ^3D_1$	2.956E+08	2.07E+08 [4b]	2.14E+08 [10]	
$3p3d\ ^3F^o_3$	$3s3d\ ^3D_2$	3.174E+08	2.19E+08 [4b]	2.25E+08 [10]	
$3p3d\ ^3F^o_4$	$3s3d\ ^3D_3$	3.794E+08	2.47E+08 [4b]	2.54E+08 [10]	
$3s4f\ ^3F^o_2$	$3s3d\ ^3D_1$	1.981E+08	1.97E+08 [4b]	1.98E+08 [10]	
$3s4f\ ^3F^o_3$	$3s3d\ ^3D_2$	2.096E+08	2.09E+08 [4b]	2.07E+08 [10]	
$3s4f\ ^3F^o_4$	$3s3d\ ^3D_3$	2.360E+08	2.35E+08 [4b]	2.33E+08 [10]	
$3s5f\ ^3F^o_2$	$3s3d\ ^3D_1$	2.801E+07	2.40E+07 [4b]	2.50E+07 [10]	
$3s5f\ ^3F^o_4$	$3s3d\ ^3D_3$	3.438E+07	2.85E+07 [4b]	2.90E+07 [10]	
$3s6f\ ^3F^o_2$	$3s3d\ ^3D_1$	1.957E+07	2.90E+07 [4b]	3.10E+07 [10]	
	$3s4d\ ^3D_1$	1.116E+07	1.07E+07 [4b]	1.00E+07 [10]	
$3s6f\ ^3F^o_3$	$3s3d\ ^3D_2$	1.910E+07	3.07E+07 [4b]	3.30E+07 [10]	
	$3s4d\ ^3D_2$	1.200E+07	1.14E+07 [4b]	1.10E+07 [10]	
$3s6f\ ^3F^o_4$	$3s3d\ ^3D_3$	1.920E+07	3.46E+07 [4b]	3.70E+07 [10]	
	$3s4d\ ^3D_3$	1.367E+07	1.28E+07 [4b]	1.20E+07 [10]	

References. [2]Present calculations; [3]Froese Fischer et al. (2006); [4b]Butler et al. (1993); [8]Vujnović et al. (2002); [10]Chang and Wang (1987); [11]Chang and Fang (1995); [12]Kernahan et al. (1979); Smith (1970); Berry et al. (1970); Head et al. (1976); [13]Träbert et al. (1999); Johnson et al. (1986).

and the ones from the CC and CI calculations is also very good for the $3s4f\ ^3F \rightarrow 3s3d\ ^3D$ transitions and fairly good for the $3s5f\ ^3F \rightarrow 3s3d\ ^3D$ transitions. On the other hand, for the $\{3p3d, 3s6f\}\ ^3F \rightarrow 3s3d\ ^3D$ transitions, the observed discrepancy between the current RCI values and the ones from the two previous calculations is substantial. This outcome indicates that the calculations by Butler et al. (1993) and Chang and Wang (1987) are insufficient to properly account for correlation and further emphasizes the quality of the present work.

In the same way as for Al I, the lifetimes of Al II excited states were also estimated based on the computed E1 transitions. In Table 9, both length τ_l and velocity τ_v forms of the currently

computed lifetimes are displayed. As already mentioned, the agreement between these two forms serves as an indication of the quality of the results. The average relative difference between the two forms is $\sim 2\%$. The largest discrepancy is observed between the length and velocity gauges of the singlet $3p^2\ ^1D$ state, as well as the singlet and triplet $3s7p\ ^{1,3}P$ states. The highest computed levels in the calculations of Al II correspond to configuration states with orbitals up to $n = 7$, such as $3s7p$. Similarly to the conclusions for the lifetimes of Al I, better agreement between the length and velocity forms of the $3s7p\ ^{1,3}P$ states could probably be obtained by including in the MR $3snl$ configurations with $n > 7$.

In Table 9, the lifetimes from the current RCI calculations are compared with results from previous MCHF-BP and BSCI calculations by Froese Fischer et al. (2006) and Chang and Fang (1995), respectively. Besides the lifetimes of the triplet $3s3p\ ^3P^o_1$ and singlet $3p^2\ ^1D_2$ states, the agreement between the RCI and MCHF-BP calculations is very good. Furthermore, the overall agreement between the RCI and BSCI calculations is sufficiently good. Despite the poor agreement between the RCI and BSCI values for the $3p^2\ ^1D_2$ state and $3s7p\ ^{1,3}P$ states, for the rest of the states the discrepancies are of the order of a few per cent. The BSCI results are more extended. However, no separate values are provided for the different LSJ-components of the triplet states and for those, the average lifetime is presented instead.

In Table 9, the theoretical lifetimes are also compared with available measurements. The measured lifetime of the $3s3p\ ^3P^o_1$ state by Träbert et al. (1999) and Johnson et al. (1986) agrees remarkably well with the calculated value by Froese Fischer et al. (2006). The agreement with the current results is fairly good too. The lifetime of the $3s3p\ ^1P^o_1$ state measured by Kernahan et al. (1979), Head et al. (1976), Berry et al. (1970) and Smith (1970) is well represented by all theoretical values. On the other hand, the results from the measurements of the $3snf\ ^3F$ states by Andersen et al. (1971) differ substantially from the theoretical RCI values. For the $3snf\ ^3F$ Rydberg series, only theoretical lifetimes using the current MCDHF and RCI approach are available. Being aware of the large uncertainties associated with early beam-foil measurements, the discrepancies between theoretical and experimental values are in some way expected. The only exception is the lifetime of the $3s5f\ ^3F$ state, which is in rather good agreement with the RCI values. In the experiments by Andersen et al. (1971) the different fine-structure components have not been separated and a single value is provided for all three different LSJ-levels.

5. Summary and conclusions

In the present work, updated and extended transition data and lifetimes are made available for both Al I and Al II. The computations of transition properties in these two systems are challenging mainly due to the strong two-electron interaction between the $3s3d\ ^1D$ and $3p^2\ ^1D$ states, which dominates the lowest part of their spectra. Thus, some of the states are strongly mixed and large amount of correlation is needed to accurately predict their LS-compositions. We are confident that in this work enough amount of correlation has been included to affirm the reliability of the results. The predicted excitation energies are in excellent agreement with the experimental data provided by the NIST database, which is a good indicator of the quality of the produced transition data and lifetimes.

We have performed an extensive comparison of the computed transition rates and lifetimes with the most recent theoretical and experimental results. There is a significant improvement in accuracy, in particular for the more complex system of neutral Al I. The computed lifetimes of Al I are in very good agreement with the measured lifetimes in high-precision laser spectroscopy experiments. The same holds for the measured lifetimes of Al II in ion storage rings. The present calculations are extended to higher energies and many of the computed transitions fall in the infrared spectral region. The new generation of telescopes are designed for this region and such transition data are of high importance. The objective of this work is to make available atomic data that could be used to improve the interpretation of abundances in stars. Lists of trustworthy elemental abundances will enable tracing stellar evolution, as well as the formation and chemical evolution of the Milky Way.

The agreement between the length and velocity gauges of the transition operator serves as a criterion to the quality of the transition data, as well as lifetimes. For most of the strong transitions in both Al I and Al II, the agreement between the two gauges is very good. For transitions involving states with the highest n quantum number for the s and p symmetries, we observe that the agreement between the length and velocity forms is less good. This becomes more evident when estimating lifetimes of excited levels that are associated with those transitions.

Acknowledgements. The authors have been supported by the Swedish Research Council (VR) under contract 2015-04842. The authors acknowledge H. Hartman, Malm University and Lund University, and H. Jnsson, Lund University, for discussions.

References

Adibekyan, V. Z., Sousa, S. G., Santos, N. C., et al. 2012, A&A, 545, A32
Andersen, T., Roberts, J. R., & Sørensen, G. 1971, Phys. Scrip., 4, 52
Bensby, T., Feltzing, S., & Oey, M. S. 2014, A&A, 562, A71
Berry, H. G., Bromander, J., & Buchta, R. 1970, Phys. Scrip., 1, 181
Butler, K., Mendoza, C., & Zeippen, C. 1993, J. Phys. B, 26, 4409
Buurman, E., Dönszelmann, A., Hansen, J. E., & Snoek, C. 1986, A&A, 164, 224
Buurman, E., & Dönszelmann, A. 1990, A&A, 227, 289
Carretta, E., Bragaglia, A., Gratton, R. G., et al. 2010, A&A, 516, A55
Chang, T. N., & Wang, R. 1987, Phys. Rev. A, 36, 3535
Chang, T. N., & Fang, T. K. 1995, Phys. Rev. A, 52, 2638
Clayton, D. D. 2003, Handbook of Isotopes in the Cosmos: Hydrogen to Gallium (Cambridge University Press)
Davidson, M. D., Volten, H., & Dönszelmann, A. 1990, A&A, 238, 452
Dyall, K. G., Grant, I. P., Johnson, C., Parpia, F. A., & Plummer, E. P. 1989, Comput. Phys. Commun., 55, 425
Ekman, J., Godefroid, M., & Hartman, H. 2014, Atoms, 2(2), 215
Froese Fischer, C., Tachiev, G., & Irimia, A. 2006, Atomic Data and Nuclear Data Tables, 92, 607-812
Froese Fischer, C. 2009, Phys. Scr. T134, 014019
Froese Fischer, C., Godefroid, M., Brage, T., Jönsson, P., & Gaigalas, G. 2016, J. Phys. B: At. Mol. Opt. Phys., 49, 182004
Gaigalas, G., Rudzikas, Z., & Froese Fischer, C. 1997, J. Phys. B: At. Mol. Opt. Phys., 30, 3747
Gaigalas, G., Fritzsche, S., & Grant, I. P. 2001, Comput. Phys. Commun., 139, 263
Gaigalas, G., Zalandauskas, T., & Rudzikas, Z. 2003, At. Data Nucl. Data Tables, 84, 99
Gaigalas, G., Zalandauskas, T., & Fritzsche, S. 2004, Comput. Phys. Commun., 157, 239
Gaigalas, G., Froese Fischer, C., Rynkun, P., & Jönsson, P. 2017, Atoms, 5(1), 6
Gehren, T., Liang, Y. C., Shi, J. R., Zhang, H. W., & Zhao, G. 2004, A&A, 413, 1045
Gehren, T., Shi, J. R., Zhang, H. W., Zhao, G. & Korn, A. J. 2006, A&A, 451, 1065
Grant, I. P. 1974, J. Phys. B, 7, 1458
Grant, I. P. 2007, Relativistic Quantum Theory of Atoms and Molecules (New York: Springer)
Head, M. E. M., Head, C. E., & Lawrence, J. N. 1976, in Atomic Structure and Lifetimes, ed. F. A. Sellin, & D. J. P egg (NY: Plenum), 147
Hibbert, A., 1989, Physica Scripta 39, 574
Johnson, B. C., Smith, P. L., & Parkinson, W. H. 1986, ApJ, 308, 1013

Jönsson, G., & Lundberg, H. 1983, Z. Phys. A, 313, 151
Jönsson, G., Kröll, S., Persson, A., & Svanberg, S. 1984, Phys. Rev. A, 30, 2429
Jönsson, P., Gaigalas, G., Bieroń, J., Froese Fischer, C., & Grant, I. P. 2013, Comput. Phys. Commun., 184, 2197
Kelleher, D. E., Podobedova, L. I. 2008a, J. Phys. Chem. Ref. Data, 37, 709
Kelleher, D. E., Podobedova, L. I. 2008b, J. Phys. Chem. Ref. Data, 37, 267
Kernahan, J. A., Pinnington, E. H., O'Neill, J. A.M, Brooks, R. L., & Donnely, K. E. 1979, Phys. Scrip., 19, 267
Kramida, A., Ralchenko, Yu., Reader, J., & NIST ASD Team 2018. *NIST Atomic Spectra Database*, ver. 5.5.3 (Online), available: `https://physics.nist.gov/asd` (2018, March 15), National Institute of Standards and Technology, Gaithersburg, MD
Lin, C. D. 1974, ApJ 187, 385
McKenzie, B. J., Grant, I. P., & Norrington, P. H. 1980, Comput. Phys.Commun., 21, 233
Mendoza, C., Eissner, W., Le Dourneuf, M., & Zeippen, C. J. 1995, J. Phys. B, 28, 3485
Mishenina, T. V., Soubiran, C., Bienaymé, O., et al. 2008, A&A, 489, 923
Nordlander, T., & Lind, K. 2017, A&A, 607, A75
Olsen, J., Roos, B. O., Jorgensen, P., Jensen, & H. J. Aa 1988, J. Chem. Phys., 89, 2185
Pehlivan Rhodin, A., Hartman, H., Nilsson, H., & Jönsson, P. 2017, A&A, 598, A102
Pehlivan Rhodin, A. 2018, 'Experimental and Computational Atomic Spectroscopy for Astrophysics: Oscillator strengths and lifetimes for Mg I, Si I, Si II, Sc I, and Sc II', Doctor, Lund Observatory, Lund
Reddy, B. E., Lambert, D. L., & Allende Prieto, C. 2006, MNRAS, 367, 1329
Smiljanic, R., Korn, A. J., Bergemann, M., Frasca, A., et al. 2014, A&A, 570, A122
Smiljanic, R., Romano, D., Bragaglia, A., Donati, P., et al. 2016, A&A, 589, A115
Smith, W. H. 1970, NIM, 90, 115
Sturesson, L., Jönsson, P., & Fischer, C. F. 2007, Comput. Phys. Commun., 177, 539
Tayal, S. S., & Hibbert, A. 1984, J. Phys. B, 17, 3835
Taylor, P. R. C. W., Bauschlicher, J., & Langhoff, S. 1988, J. Phys. B, 21, L333
Theodosiou, C. E. 1992, Phys. Rev. A, 45, 7756
Trefftz, E. 1988, J. Phys. B: At. Mol. Opt. Phys., 21, 1761
Träbert, E., Wolf, A., & Linkemann, J. 1999, J. Phys. B, 32, 637
Vujnović, V., Blagoev, K., Fürböck, C., Neger, T., & Jäger, H. 2002, A&A, 338, 704
Weiss, A. W. 1974, Phys. Rev., 9, 1524
Wiese, W. L., Smith, M. W., & Miles, B. M. 1969, NSRDS-NBS 22, Vol. 2, 47
Wiese, W. L., & Martin, G. A. 1980, Transition Probabilities, Part II, Vol. Natl. Stand. Ref. Data System., Natl. Bur. Std. 68 (Washington DC)

Table 8: Computed excitation energies in cm^{-1} for the 78 lowest states in Al II. The energies are given as a function of the increasing active set of orbitals, accounting for VV correlation, where n indicates the maximum principle quantum number of the orbitals included in the active set. In the third last column, the final energy values are displayed after accounting for CV correlation. The differences ΔE between the final computations and the observed values are shown in the last column. The sequence and naming of the configurations and $LS\,J$-levels are in accordance with the final (CV) computed energies. The levels of the singlet and triplet $3s6h\ ^{1,3}H$, as well as the $3p3d\ ^1D$ level have not yet been observed and thus, no ΔE values are available for those.

			VV								
Pos.	Conf.	$LS\,J$	$n = 8$	$n = 9$	$n = 10$	$n = 11$	$n = 12$	$n = 13$	CV	E_{obs} [1]	ΔE
1	$3s^2$	$^1S_0$	0	0	0	0	0	0	0	0	0
2	$3s\,3p$	$^3P^o_0$	36 227	36 280	36 298	36 318	36 332	36 335	37 445	37 393	-52
3		$^3P^o_1$	36 286	36 339	36 357	36 377	36 391	36 394	37 503	37 454	-49
4		$^3P^o_2$	36 405	36 459	36 477	36 496	36 511	36 514	37 626	37 578	-48
5		$^1P^o_1$	59 810	59 698	59 617	59 619	59 606	59 602	59 982	59 852	-130
6	$3p^2$	$^1D_2$	83 542	83 596	83 620	83 641	83 657	83 660	85 692	85 481	-211
7	$3s\,4s$	$^3S_1$	89 965	90 028	90 059	90 082	90 099	90 102	91 425	91 275	-150
8	$3p^2$	$^3P_0$	92 679	92 709	92 716	92 736	92 750	92 752	94 211	94 085	-126
9		$^3P_1$	92 739	92 769	92 776	92 795	92 809	92 812	94 264	94 147	-117
10		$^3P_2$	92 855	92 885	92 892	92 912	92 926	92 928	94 375	94 269	-106
11	$3s\,4s$	$^1S_0$	94 003	94 057	94 084	94 101	94 111	94 114	95 543	95 351	-192
12	$3s\,3d$	$^3D_2$	94 262	94 243	94 241	94 262	94 278	94 280	95 791	95 549	-242
13		$^3D_1$	94 261	94 243	94 242	94 263	94 279	94 281	95 794	95 551	-243
14		$^3D_3$	94 263	94 242	94 239	94 261	94 276	94 279	95 804	95 551	-253
15	$3s\,4p$	$^3P^o_0$	103 935	104 003	104 030	104 053	104 070	104 073	105 582	105 428	-154
16		$^3P^o_1$	103 948	104 017	104 044	104 067	104 084	104 087	105 594	105 442	-152
17		$^3P^o_2$	103 976	104 045	104 073	104 095	104 112	104 115	105 623	105 471	-152
18		$^1P^o_1$	105 597	105 643	105 655	105 673	105 683	105 685	107 132	106 921	-211
19	$3s\,3d$	$^1D_2$	109 010	108 919	108 897	108 910	108 918	108 918	110 330	110 090	-240
20	$3p^2$	$^1S_0$	111 100	110 804	110 659	110 643	110 618	110 608	112 086	111 637	-449
21	$3s\,5s$	$^3S_1$	118 564	118 632	118 661	118 685	118 702	118 705	120 259	120 093	-166
22		$^1S_0$	119 807	119 878	119 908	119 931	119 946	119 948	121 544	121 367	-177
23	$3s\,4d$	$^3D_2$	120 013	120 034	120 045	120 068	120 085	120 088	121 684	121 484	-200
24		$^3D_1$	120 013	120 034	120 046	120 068	120 085	120 088	121 685	121 484	-201
25		$^3D_3$	120 014	120 034	120 045	120 068	120 084	120 087	121 688	121 484	-204
26	$3s\,4f$	$^3F^o_2$	121 657	121 739	121 772	121 797	121 815	121 818	123 606	123 418	-188
27		$^3F^o_3$	121 659	121 742	121 775	121 799	121 817	121 820	123 608	123 420	-188
28		$^3F^o_4$	121 663	121 745	121 778	121 802	121 820	121 824	123 612	123 423	-189
29		$^1F^o_3$	121 735	121 818	121 852	121 876	121 894	121 898	123 657	123 471	-186
30	$3s\,4d$	$^1D_2$	123 606	123 489	123 461	123 473	123 482	123 483	125 049	124 794	-255
31	$3s\,5p$	$^3P^o_0$	124 108	124 185	124 212	124 236	124 254	124 257	125 869	125 703	-166
32		$^3P^o_1$	124 114	124 190	124 218	124 242	124 259	124 262	125 874	125 709	-165
33		$^3P^o_2$	124 126	124 203	124 231	124 254	124 272	124 275	125 887	125 722	-165
34		$^1P^o_1$	124 302	124 375	124 401	124 424	124 440	124 443	126 078	125 869	-209
35	$3s\,6s$	$^3S_1$	130 615	130 689	130 716	130 740	130 758	130 761	132 386	132 216	-170
36		$^1S_0$	131 160	131 237	131 268	131 291	131 308	131 311	132 953	132 779	-174
37	$3s\,5d$	$^3D_2$	131 265	131 307	131 326	131 348	131 365	131 368	133 013	132 823	-190
38		$^3D_1$	131 265	131 307	131 327	131 348	131 365	131 368	133 013	132 823	-190
39		$^3D_3$	131 266	131 307	131 326	131 347	131 365	131 368	133 017	132 823	-194
40	$3s\,5f$	$^3F^o_2$	131 641	131 712	131 745	131 769	131 787	131 790	133 639	133 438	-201
41		$^3F^o_3$	131 647	131 718	131 751	131 776	131 794	131 797	133 644	133 443	-201
42		$^3F^o_4$	131 655	131 727	131 760	131 785	131 803	131 806	133 654	133 450	-204
43		$^1F^o_3$	131 968	132 048	132 082	132 106	132 124	132 128	133 866	133 682	-184
44	$3s\,5d$	$^1D_2$	132 490	132 447	132 445	132 460	132 474	132 476	134 143	133 916	-227
45	$3s\,5g$	$^3G_3$	132 487	132 577	132 611	132 636	132 654	132 657	134 359	134 184	-175
46		$^3G_4$	132 487	132 577	132 611	132 636	132 654	132 658	134 360	134 184	-176
47		$^3G_5$	132 487	132 577	132 611	132 636	132 654	132 657	134 360	134 184	-176
48		$^1G_4$	132 487	132 577	132 611	132 636	132 654	132 658	134 360	134 184	-176
49	$3s\,6p$	$^1P^o_1$	133 288	133 366	133 387	133 411	133 428	133 431	135 132	134 919	-213
50		$^3P^o_0$	133 378	133 459	133 485	133 509	133 526	133 530	135 183	135 012	-171

Table 8: continued.

			VV								
Pos.	Conf.	LSJ	$n = 8$	$n = 9$	$n = 10$	$n = 11$	$n = 12$	$n = 13$	CV	$E_{\rm obs}$ [(1)]	ΔE
51		$^3P^o_1$	133 381	133 462	133 488	133 512	133 530	133 533	135 186	135 016	-170
52		$^3P^o_2$	133 388	133 468	133 494	133 518	133 536	133 539	135 192	135 022	-170
53	$3s\,7s$	$^3S_1$	136 870	136 949	136 975	136 999	137 014	137 017	138 675	138 500	-175
54	$3s\,6f$	$^3F^o_2$	136 665	136 628	136 655	136 678	136 695	136 698	138 810	138 521	-289
55		$^3F^o_3$	136 684	136 649	136 677	136 699	136 717	136 720	138 829	138 539	-290
56		$^3F^o_4$	136 709	136 677	136 704	136 727	136 745	136 748	138 862	138 562	-300
57	$3s\,7s$	$^1S_0$	137 154	137 236	137 267	137 291	137 307	137 311	138 974	138 801	-173
58	$3s\,6d$	$^3D_2$	137 217	137 273	137 297	137 314	137 331	137 333	139 005	138 815	-190
59		$^3D_1$	137 217	137 273	137 297	137 314	137 331	137 333	139 005	138 815	-190
60		$^3D_3$	137 218	137 273	137 297	137 314	137 331	137 333	139 010	138 815	-195
61	$3s\,6f$	$^1F^o_3$	137 562	137 625	137 657	137 681	137 699	137 702	139 437	139 245	-192
62	$3s\,6d$	$^1D_2$	137 753	137 754	137 767	137 786	137 801	137 803	139 497	139 289	-208
63	$3s\,6g$	$^3G_3$	137 898	137 988	138 022	138 046	138 065	138 067	139 766	139 591	-175
64		$^3G_4$	137 898	137 988	138 022	138 046	138 065	138 068	139 766	139 591	-175
65		$^3G_5$	137 898	137 988	138 022	138 046	138 065	138 067	139 766	139 591	-175
66		$^1G_4$	137 898	137 988	138 022	138 047	138 065	138 068	139 766	139 591	-175
67	$3s\,6h$	$^3H^o_4$	137 965	138 043	138 079	138 103	138 121	138 125	139 817		
68		$^3H^o_5$	137 965	138 043	138 079	138 103	138 121	138 125	139 817		
69		$^1H^o_5$	137 965	138 043	138 079	138 103	138 121	138 125	139 817		
70		$^3H^o_6$	137 965	138 043	138 079	138 103	138 121	138 125	139 817		
71	$3s\,7p$	$^1P^o_1$	138 286	138 364	138 360	138 384	138 401	138 402	140 148	139 919	-229
72		$^3P^o_0$	138 439	138 522	138 545	138 569	138 587	138 589	140 266	140 090	-176
73		$^3P^o_1$	138 441	138 524	138 547	138 571	138 589	138 591	140 268	140 092	-176
74		$^3P^o_2$	138 445	138 529	138 552	138 575	138 593	138 595	140 272	140 096	-176
75	$3p\,3d$	$^3F^o_2$	136 665	136 628	136 655	136 678	136 695	139 291	141 615	141 085	-531
76		$^3F^o_3$	136 684	136 649	136 677	136 699	136 717	139 311	141 665	141 110	-555
77		$^3F^o_4$	136 709	136 677	136 704	136 727	136 745	139 338	141 768	141 143	-625
78	$3p\,3d$	$^1D^o_2$	140 333	140 372	140 385	140 408	140 425	140 428	142 964		

References. [(1)]NIST Atomic Spectra Database 2018 (Kramida et al. 2018).

Table 9: Comparison between computed and observed lifetimes τ in seconds, for 75 excited states in Al II. For the current RCI calculations both length τ_l and velocity τ_v forms are displayed. In the third and second last columns, the predicted lifetimes from MCHF-BP and BSCI calculations are, respectively, given in length form. The last column contains available lifetimes from experimental measurements, together with their uncertainties.

			RCI [(2)]		MCHF-BP [(3)]	BSCI [(11)]	Expt.[(12),(13),(14)]
Pos.	Conf.	LSJ	τ_l	τ_v	τ_l		τ
1	$3s3p$	$^3P^o_1$	3.274E-04	2.965E-04	3.051E-04		3.02 (2) E-04 [(13)]
2		$^1P^o_1$	7.120E-10	7.089E-10	7.141E-10	6.70 E-10	6.90(13)E-10 [(12)]
3	$3p^2$	$^1D_2$	3.351E-06	2.630E-06	2.270E-06	2.51 E-06	
4	$3s4s$	$^3S_1$	1.318E-09	1.325E-09	1.322E-09	1.32 E-09	
5	$3p^2$	$^3P_0$	8.091E-10	8.032E-10	8.098E-10		
6		$^3P_1$	8.081E-10	8.023E-10	8.082E-10		
7		$^3P_2$	8.059E-10	8.000E-10	8.054E-10		
8	$3s4s$	$^1S_0$	2.921E-09	2.922E-09	2.893E-09	2.93 E-09	
9	$3s3d$	$^3D_2$	8.337E-10	8.346E-10	8.252E-10	8.00 E-10	
10		$^3D_1$	8.319E-10	8.328E-10	8.233E-10	8.00 E-10	
11		$^3D_3$	8.358E-10	8.357E-10	8.277E-10	8.00 E-10	
12	$3s4p$	$^3P^o_0$	1.390E-08	1.394E-08	1.384E-08	1.403E-08	
13		$^3P^o_1$	1.386E-08	1.391E-08	1.379E-08	1.403E-08	
14		$^3P^o_2$	1.379E-08	1.384E-08	1.369E-08	1.403E-08	

Table 9: continued.

			RCI [2]		MCHF-BP [3]	BSCI [11]	Expt.[12],[13],[14]
Pos.	Conf.	LSJ	τ_l	τ_v	τ_l		$\tau_{\rm obs}$
15		$^1P^o_1$	1.099E-08	1.113E-08	1.116E-08	1.007E-08	
16	$3s3d$	$^1D_2$	7.204E-10	7.192E-10	6.994E-10	7.20 E-10	
17	$3p^2$	$^1S_0$	9.804E-10	9.758E-10	9.720E-10	9.50 E-10	
18	$3s5s$	$^3S_1$	2.767E-09	2.785E-09		2.78 E-09	
19		$^1S_0$	4.059E-09	4.055E-09		4.33 E-09	
20	$3s4d$	$^3D_2$	3.862E-09	3.872E-09		3.71 E-09	
21		$^3D_1$	3.850E-09	3.860E-09		3.71 E-09	
22		$^3D_3$	3.880E-09	3.889E-09		3.71 E-09	
23	$3s4f$	$^3F^o_2$	4.235E-09	4.254E-09			6.4 (5)E-09 [14]
24		$^3F^o_3$	4.230E-09	4.248E-09			6.4 (5)E-09 [14]
25		$^3F^o_4$	4.230E-09	4.256E-09			6.4 (5)E-09 [14]
26		$^1F^o_3$	3.428E-09	3.438E-09			
27	$3s4d$	$^1D_2$	1.366E-09	1.368E-09		1.31 E-09	
28	$3s5p$	$^3P^o_0$	4.903E-08	4.941E-08		4.928E-08	
29		$^3P^o_1$	4.862E-08	4.899E-08		4.928E-08	
30		$^3P^o_2$	4.850E-08	4.903E-08		4.928E-08	
31		$^1P^o_1$	1.315E-08	1.377E-08		1.263E-08	
32	$3s6s$	$^3S_1$	5.196E-09	5.242E-09		5.19 E-09	
33		$^1S_0$	7.265E-09	7.254E-09		7.61 E-09	
34	$3s5d$	$^3D_2$	1.077E-08	1.081E-08		1.03 E-08	
35		$^3D_1$	1.073E-08	1.077E-08		1.03 E-08	
36		$^3D_3$	1.085E-08	1.090E-08		1.03 E-08	
37	$3s5f$	$^3F^o_2$	1.337E-08	1.356E-08			1.4 (2)E-08 [14]
38		$^3F^o_3$	1.328E-08	1.348E-08			1.4 (2)E-08 [14]
39		$^3F^o_4$	1.320E-08	1.345E-08			1.4 (2)E-08 [14]
40		$^1F^o_3$	5.981E-09	6.015E-09			
41	$3s5d$	$^1D_2$	3.523E-09	3.525E-09		3.37 E-09	
42	$3s5g$	$^3G_3$	1.389E-08	1.390E-08			
43		$^3G_4$	1.389E-08	1.389E-08			
44		$^3G_5$	1.389E-08	1.390E-08			
45		$^1G_4$	1.383E-08	1.384E-08			
46	$3s6p$	$^1P^o_1$	1.322E-08	1.425E-08		1.211E-08	
47		$^3P^o_0$	1.147E-07	1.171E-07		1.105E-07	
48		$^3P^o_1$	1.097E-07	1.122E-07		1.105E-07	
49		$^3P^o_2$	1.137E-07	1.173E-07		1.105E-07	
50	$3s7s$	$^3S_1$	9.039E-09	9.167E-09		8.78 E-09	
51	$3s6f$	$^3F^o_2$	2.041E-08	2.051E-08			1.5 (1)E-08 [14]
52		$^3F^o_3$	2.111E-08	2.125E-08			1.5 (1)E-08 [14]
53		$^3F^o_4$	2.222E-08	2.236E-08			1.5 (1)E-08 [14]
54	$3s7s$	$^1S_0$	1.174E-08	1.170E-08			
55	$3s6d$	$^3D_2$	2.386E-08	2.399E-08		2.234E-08	
56		$^3D_1$	2.376E-08	2.391E-08		2.234E-08	
57		$^3D_3$	2.423E-08	2.445E-08		2.234E-08	
58	$3s6f$	$^1F^o_3$	9.655E-09	9.720E-09			
59	$3s6d$	$^1D_2$	7.546E-09	7.518E-09		7.46 E-09	
60	$3s6g$	$^3G_3$	2.415E-08	2.417E-08			
61		$^3G_4$	2.412E-08	2.413E-08			
62		$^3G_5$	2.417E-08	2.415E-08			
63		$^1G_4$	2.373E-08	2.375E-08			
64	$3s6h$	$^3H^o_4$	3.753E-08	3.759E-08			
65		$^3H^o_5$	3.753E-08	3.759E-08			
66		$^1H^o_5$	3.753E-08	3.759E-08			
67		$^1H^o_6$	3.753E-08	3.759E-08			
68	$3s7p$	$^1P^o_1$	1.238E-08	1.450E-08		1.081E-08	
69		$^3P^o_0$	1.904E-07	2.090E-07		1.608E-07	

Table 9: continued.

Pos.	Conf.	LSJ	RCI [2] τ_l	RCI [2] τ_v	MCHF-BP [3] τ_l	BSCI [11]	Expt.[12],[13],[14] $\tau_{\rm obs}$
70		$^3P^o_1$	1.897E-07	2.078E-07		1.608E-07	
71		$^3P^o_2$	1.865E-07	2.148E-07		1.608E-07	
72	$3p3d$	$^3F^o_2$	2.769E-09	2.735E-09			3.5 (3)E-09 [14]
73		$^3F^o_3$	2.736E-09	2.701E-09			3.5 (3)E-09 [14]
74		$^3F^o_4$	2.586E-09	2.539E-09			3.5 (3)E-09 [14]
75		$^1D^o_2$	8.207E-10	8.198E-10			

References. [2]present calculations; [3]Froese Fischer et al. (2006); [11]Chang and Fang (1995); [12]Kernahan et al. (1979); Smith (1970); Berry et al. (1970); Head et al. (1976); [13]Träbert et al. (1999); Johnson et al. (1986); [14]Andersen et al. (1971).

Table 10: Transition data for Al I

Upper	Lower	ΔE (cm^{-1})	λ (Å)	A(s^{-1})	gf
$3s^2\,5d\,^2D_{3/2}$	$3s^2\,3p\,^2P^o_{1/2}$	44125	2266.251	8.20E+07	2.53E-01
$3s^2\,5d\,^2D_{5/2}$	$3s^2\,3p\,^2P^o_{3/2}$	44025	2271.420	9.71E+07	4.50E-01
$3s^2\,5d\,^2D_{3/2}$	$3s^2\,3p\,^2P^o_{3/2}$	44021	2271.613	1.60E+07	4.94E-02
$3s^2\,4d\,^2D_{3/2\,b}$	$3s^2\,3p\,^2P^o_{1/2}$	42232	2367.863	7.13E+07	2.40E-01
$3s^2\,4d\,^2D_{5/2\,b}$	$3s^2\,3p\,^2P^o_{3/2}$	42132	2373.437	8.41E+07	4.26E-01
$3s^2\,4d\,^2D_{3/2\,b}$	$3s^2\,3p\,^2P^o_{3/2}$	42128	2373.717	1.39E+07	4.69E-02
$3s^2\,6s\,^2S_{1/2}$	$3s^2\,3p\,^2P^o_{1/2}$	41963	2383.014	4.83E+06	8.22E-03
$3s^2\,6s\,^2S_{1/2}$	$3s^2\,3p\,^2P^o_{3/2}$	41859	2388.943	9.58E+06	1.64E-02
$3s^2\,4d\,^2D_{3/2\,a}$	$3s^2\,3p\,^2P^o_{1/2}$	38951	2567.300	1.72E+07	6.81E-02
$3s^2\,4d\,^2D_{5/2\,a}$	$3s^2\,3p\,^2P^o_{3/2}$	38852	2573.839	2.01E+07	1.20E-01
$3s^2\,4d\,^2D_{3/2\,a}$	$3s^2\,3p\,^2P^o_{3/2}$	38847	2574.183	3.29E+06	1.31E-02
$3s^2\,5s\,^2S_{1/2}$	$3s^2\,3p\,^2P^o_{1/2}$	37511	2665.844	1.28E+07	2.72E-02
$3s^2\,5s\,^2S_{1/2}$	$3s^2\,3p\,^2P^o_{3/2}$	37407	2673.266	2.53E+07	5.43E-02
$3s^2\,3d\,^2D_{3/2}$	$3s^2\,3p\,^2P^o_{1/2}$	32414	3085.076	6.54E+07	3.73E-01
$3s^2\,3d\,^2D_{5/2}$	$3s^2\,3p\,^2P^o_{3/2}$	32311	3094.829	7.88E+07	6.79E-01
$3s^2\,3d\,^2D_{3/2}$	$3s^2\,3p\,^2P^o_{3/2}$	32309	3095.021	1.32E+07	7.59E-02
$3s\,3p^2\,^4P_{3/2}$	$3s^2\,3p\,^2P^o_{1/2}$	28907	3459.365	1.08E+02	7.76E-07
$3s\,3p^2\,^4P_{5/2}$	$3s^2\,3p\,^2P^o_{3/2}$	28876	3463.019	3.84E+02	4.14E-06
$3s\,3p^2\,^4P_{1/2}$	$3s^2\,3p\,^2P^o_{1/2}$	28862	3464.703	1.99E+02	7.16E-07
$3s\,3p^2\,^4P_{3/2}$	$3s^2\,3p\,^2P^o_{3/2}$	28802	3471.874	4.11E+01	2.97E-07
$3s\,3p^2\,^4P_{1/2}$	$3s^2\,3p\,^2P^o_{3/2}$	28758	3477.250	4.07E+02	1.47E-06
$3s^2\,4s\,^2S_{1/2}$	$3s^2\,3p\,^2P^o_{1/2}$	25196	3968.882	4.97E+07	2.35E-01
$3s^2\,4s\,^2S_{1/2}$	$3s^2\,3p\,^2P^o_{3/2}$	25091	3985.356	9.88E+07	4.71E-01
$3s^2\,6p\,^2P^o_{3/2}$	$3s^2\,4s\,^2S_{1/2}$	17965	5566.147	4.00E+05	7.44E-03
$3s^2\,6p\,^2P^o_{1/2}$	$3s^2\,4s\,^2S_{1/2}$	17963	5566.742	3.91E+05	3.63E-03
$3s^2\,5p\,^2P^o_{3/2}$	$3s^2\,4s\,^2S_{1/2}$	14909	6706.913	1.18E+06	3.17E-02
$3s^2\,5p\,^2P^o_{1/2}$	$3s^2\,4s\,^2S_{1/2}$	14905	6708.987	1.15E+06	1.56E-02
$3s^2\,5d\,^2D_{3/2}$	$3s^2\,4p\,^2P^o_{1/2}$	11325	8829.866	6.03E+04	2.82E-03
$3s^2\,5d\,^2D_{5/2}$	$3s^2\,4p\,^2P^o_{3/2}$	11314	8837.834	7.73E+04	5.43E-03
$3s^2\,5d\,^2D_{3/2}$	$3s^2\,4p\,^2P^o_{3/2}$	11311	8840.756	1.40E+04	6.54E-04
$3s^2\,5f\,^2F^o_{5/2}$	$3s^2\,3d\,^2D_{3/2}$	11246	8892.051	6.63E+06	4.72E-01
$3s^2\,5f\,^2F^o_{5/2}$	$3s^2\,3d\,^2D_{5/2}$	11244	8893.632	4.74E+05	3.37E-02
$3s^2\,5f\,^2F^o_{7/2}$	$3s^2\,3d\,^2D_{5/2}$	11243	8893.640	7.11E+06	6.74E-01
$3s^2\,6p\,^2P^o_{3/2}$	$3s^2\,3d\,^2D_{3/2}$	10747	9304.360	3.41E+02	1.77E-05

Table 10: Continued.

Upper	Lower	ΔE (cm^{-1})	λ (Å)	A(s^{-1})	gf
$3s^2\,6p\,^2P^o_{1/2}$	$3s^2\,3d\,^2D_{3/2}$	10745	9306.022	3.15E+03	8.18E-05
$3s^2\,6p\,^2P^o_{3/2}$	$3s^2\,3d\,^2D_{5/2}$	10745	9306.091	3.14E+03	1.63E-04
$3s^2\,4d\,^2D_{3/2\,b}$	$3s^2\,4p\,^2P^o_{1/2}$	9431	10602.599	4.45E+05	3.00E-02
$3s^2\,4d\,^2D_{5/2\,b}$	$3s^2\,4p\,^2P^o_{3/2}$	9422	10612.714	5.37E+05	5.44E-02
$3s^2\,4d\,^2D_{3/2\,b}$	$3s^2\,4p\,^2P^o_{3/2}$	9417	10618.293	8.69E+04	5.87E-03
$3s^2\,6s\,^2S_{1/2}$	$3s^2\,4p\,^2P^o_{1/2}$	9163	10913.290	1.23E+06	4.37E-02
$3s^2\,6s\,^2S_{1/2}$	$3s^2\,4p\,^2P^o_{3/2}$	9149	10929.929	2.43E+06	8.70E-02
$3s^2\,4f\,^2F^o_{5/2}$	$3s^2\,3d\,^2D_{3/2}$	8748	11430.296	1.37E+07	1.61E+00
$3s^2\,4f\,^2F^o_{7/2}$	$3s^2\,3d\,^2D_{5/2}$	8746	11432.896	1.47E+07	2.30E+00
$3s^2\,4f\,^2F^o_{5/2}$	$3s^2\,3d\,^2D_{5/2}$	8746	11432.909	9.78E+05	1.15E-01
$3s^2\,5p\,^2P^o_{3/2}$	$3s^2\,3d\,^2D_{3/2}$	7691	13000.706	4.90E+03	4.97E-04
$3s^2\,5p\,^2P^o_{3/2}$	$3s^2\,3d\,^2D_{5/2}$	7689	13004.087	4.42E+04	4.49E-03
$3s^2\,5p\,^2P^o_{1/2}$	$3s^2\,3d\,^2D_{3/2}$	7687	13008.502	5.09E+04	2.58E-03
$3s^2\,4p\,^2P^o_{3/2}$	$3s^2\,4s\,^2S_{1/2}$	7618	13125.995	1.59E+07	1.64E+00
$3s^2\,4p\,^2P^o_{1/2}$	$3s^2\,4s\,^2S_{1/2}$	7604	13150.057	1.58E+07	8.19E-01
$3s^2\,4d\,^2D_{3/2\,a}$	$3s^2\,4p\,^2P^o_{1/2}$	6150	16257.810	9.65E+06	1.53E+00
$3s^2\,4d\,^2D_{5/2\,a}$	$3s^2\,4p\,^2P^o_{3/2}$	6142	16280.970	1.16E+07	2.76E+00
$3s^2\,4d\,^2D_{3/2\,a}$	$3s^2\,4p\,^2P^o_{3/2}$	6136	16294.739	1.92E+06	3.06E-01
$3s^2\,6p\,^2P^o_{3/2}$	$3s^2\,5s\,^2S_{1/2}$	5650	17698.520	4.47E+05	8.39E-02
$3s^2\,6p\,^2P^o_{1/2}$	$3s^2\,5s\,^2S_{1/2}$	5648	17704.536	4.41E+05	4.14E-02
$3s^2\,5s\,^2S_{1/2}$	$3s^2\,4p\,^2P^o_{1/2}$	4711	21226.781	3.82E+06	5.15E-01
$3s^2\,5f\,^2F^o_{5/2}$	$3s^2\,4d\,^2D_{3/2\,a}$	4708	21237.329	8.28E+04	3.36E-02
$3s^2\,5f\,^2F^o_{5/2}$	$3s^2\,4d\,^2D_{5/2\,a}$	4703	21260.808	6.08E+03	2.47E-03
$3s^2\,5f\,^2F^o_{7/2}$	$3s^2\,4d\,^2D_{5/2\,a}$	4703	21260.854	9.12E+04	4.94E-02
$3s^2\,5s\,^2S_{1/2}$	$3s^2\,4p\,^2P^o_{3/2}$	4697	21289.777	7.60E+06	1.03E+00
$3s^2\,6p\,^2P^o_{3/2}$	$3s^2\,4d\,^2D_{3/2\,a}$	4210	23751.107	9.48E+03	3.21E-03
$3s^2\,6p\,^2P^o_{1/2}$	$3s^2\,4d\,^2D_{3/2\,a}$	4208	23761.943	9.32E+04	1.58E-02
$3s^2\,6p\,^2P^o_{3/2}$	$3s^2\,4d\,^2D_{5/2\,a}$	4205	23780.421	8.43E+04	2.86E-02
$3s^2\,5d\,^2D_{3/2}$	$3s^2\,5p\,^2P^o_{1/2}$	4024	24848.795	1.41E+05	5.22E-02
$3s^2\,5d\,^2D_{5/2}$	$3s^2\,5p\,^2P^o_{3/2}$	4023	24854.168	1.67E+05	9.29E-02
$3s^2\,5d\,^2D_{3/2}$	$3s^2\,5p\,^2P^o_{3/2}$	4019	24877.293	2.68E+04	9.96E-03
$3s^2\,5d\,^2D_{5/2}$	$3s^2\,4f\,^2F^o_{7/2}$	2966	33707.827	2.33E+04	2.39E-02
$3s^2\,5d\,^2D_{3/2}$	$3s^2\,4f\,^2F^o_{5/2}$	2962	33750.262	2.37E+04	1.62E-02
$3s^2\,5p\,^2P^o_{3/2}$	$3s^2\,5s\,^2S_{1/2}$	2594	38544.112	2.58E+06	2.30E+00
$3s^2\,5p\,^2P^o_{1/2}$	$3s^2\,5s\,^2S_{1/2}$	2589	38612.722	2.57E+06	1.15E+00
$3s^2\,5g\,^2G_{7/2}$	$3s^2\,4f\,^2F^o_{5/2}$	2524	39616.041	4.19E+06	7.89E+00
$3s^2\,5g\,^2G_{9/2}$	$3s^2\,4f\,^2F^o_{7/2}$	2524	39616.041	4.35E+06	1.02E+01
$3s^2\,5g\,^2G_{7/2}$	$3s^2\,4f\,^2F^o_{7/2}$	2524	39616.041	1.55E+05	2.92E-01
$3s^2\,4f\,^2F^o_{5/2}$	$3s^2\,4d\,^2D_{3/2\,a}$	2211	45220.836	1.77E+06	3.26E+00
$3s^2\,4f\,^2F^o_{7/2}$	$3s^2\,4d\,^2D_{5/2\,a}$	2206	45327.217	1.89E+06	4.65E+00
$3s^2\,4f\,^2F^o_{5/2}$	$3s^2\,4d\,^2D_{5/2\,a}$	2206	45327.423	1.26E+05	2.32E-01
$3s^2\,4d\,^2D_{5/2\,b}$	$3s^2\,5p\,^2P^o_{3/2}$	2131	46923.243	2.16E+06	4.28E+00
$3s^2\,4d\,^2D_{3/2\,b}$	$3s^2\,5p\,^2P^o_{1/2}$	2130	46930.730	1.80E+06	2.38E+00
$3s^2\,4d\,^2D_{3/2\,b}$	$3s^2\,5p\,^2P^o_{3/2}$	2126	47032.707	3.58E+05	4.75E-01
$3s^2\,6s\,^2S_{1/2}$	$3s^2\,5p\,^2P^o_{1/2}$	1862	53697.618	9.10E+05	7.87E-01
$3s^2\,6s\,^2S_{1/2}$	$3s^2\,5p\,^2P^o_{3/2}$	1857	53830.874	1.81E+06	1.57E+00
$3s^2\,5f\,^2F^o_{5/2}$	$3s^2\,4d\,^2D_{3/2\,b}$	1427	70031.444	1.23E+06	5.41E+00
$3s^2\,5f\,^2F^o_{7/2}$	$3s^2\,4d\,^2D_{5/2\,b}$	1422	70275.550	1.31E+06	7.74E+00
$3s^2\,5f\,^2F^o_{5/2}$	$3s^2\,4d\,^2D_{5/2\,b}$	1422	70275.550	8.71E+04	3.87E-01
$3s^2\,6p\,^2P^o_{3/2}$	$3s^2\,6s\,^2S_{1/2}$	1198	83466.184	7.28E+05	3.04E+00
$3s^2\,6p\,^2P^o_{1/2}$	$3s^2\,6s\,^2S_{1/2}$	1196	83600.157	7.26E+05	1.52E+00

Table 10: Continued.

Upper	Lower	ΔE (cm^{-1})	λ (Å)	A(s^{-1})	gf
$3s^2\,5p\,^2P^o_{3/2}$	$3s^2\,4d\,^2D_{3/2\,a}$	1154	86612.332	3.19E+04	1.44E-01
$3s^2\,5p\,^2P^o_{1/2}$	$3s^2\,4d\,^2D_{3/2\,a}$	1149	86959.546	3.16E+05	7.16E-01
$3s^2\,5p\,^2P^o_{3/2}$	$3s^2\,4d\,^2D_{5/2\,a}$	1149	87003.428	2.85E+05	1.29E+00
$3s^2\,4d\,^2D_{5/2\,b}$	$3s^2\,4f\,^2F^o_{7/2}$	1074	93080.403	1.72E+05	1.34E+00
$3s^2\,4d\,^2D_{3/2\,b}$	$3s^2\,4f\,^2F^o_{5/2}$	1069	93511.254	1.79E+05	9.37E-01
$3s^2\,5d\,^2D_{5/2}$	$3s^2\,6p\,^2P^o_{3/2}$	967	103336.743	6.31E+05	6.06E+00
$3s^2\,5d\,^2D_{3/2}$	$3s^2\,6p\,^2P^o_{1/2}$	965	103531.458	5.25E+05	3.38E+00
$3s^2\,5d\,^2D_{3/2}$	$3s^2\,6p\,^2P^o_{3/2}$	963	103737.668	1.04E+05	6.73E-01
$3s^2\,6p\,^2P^o_{3/2}$	$3s^2\,4d\,^2D_{3/2\,b}$	929	107575.464	3.95E+04	2.74E-01
$3s^2\,6p\,^2P^o_{1/2}$	$3s^2\,4d\,^2D_{3/2\,b}$	927	107798.116	3.93E+05	1.37E+00
$3s^2\,6p\,^2P^o_{3/2}$	$3s^2\,4d\,^2D_{5/2\,b}$	924	108152.538	3.52E+05	2.47E+00
$3s^2\,5d\,^2D_{5/2}$	$3s^2\,5f\,^2F^o_{7/2}$	469	213056.076	7.01E+04	2.86E+00
$3s^2\,5d\,^2D_{3/2}$	$3s^2\,5f\,^2F^o_{5/2}$	465	214767.407	7.21E+04	2.00E+00
$3s^2\,4p\,^2P^o_{3/2}$	$3s^2\,3d\,^2D_{5/2}$	398	251022.918	3.25E+03	1.23E-01
$3s^2\,4p\,^2P^o_{1/2}$	$3s^2\,3d\,^2D_{3/2}$	386	258779.080	3.30E+03	6.62E-02

Table 11: Transition data for Al II

Upper	Lower	ΔE (cm^{-1})	λ (Å)	A(s^{-1})	gf
$3s\,7p\,^1P^o_1$	$3s^2\,^1S_0$	140148	713.529	8.07E+06	1.85E-03
$3s\,6p\,^3P^o_1$	$3s^2\,^1S_0$	135186	739.718	3.30E+04	8.12E-06
$3s\,6p\,^1P^o_1$	$3s^2\,^1S_0$	135132	740.013	8.37E+06	2.06E-03
$3s\,5p\,^1P^o_1$	$3s^2\,^1S_0$	126078	793.158	6.16E+06	1.74E-03
$3s\,5p\,^3P^o_1$	$3s^2\,^1S_0$	125874	794.443	2.44E+04	6.92E-06
$3s\,4p\,^1P^o_1$	$3s^2\,^1S_0$	107132	933.420	1.53E+06	5.99E-04
$3s\,6d\,^3D_1$	$3s\,3p\,^3P^o_0$	101560	984.639	8.34E+06	3.64E-03
$3s\,6d\,^3D_1$	$3s\,3p\,^3P^o_1$	101501	985.205	6.19E+06	2.70E-03
$3s\,6d\,^3D_2$	$3s\,3p\,^3P^o_1$	101501	985.209	1.12E+07	8.14E-03
$3s\,6d\,^3D_3$	$3s\,3p\,^3P^o_2$	101383	986.354	1.45E+07	1.48E-02
$3s\,6d\,^3D_1$	$3s\,3p\,^3P^o_2$	101378	986.402	4.07E+05	1.78E-04
$3s\,6d\,^3D_2$	$3s\,3p\,^3P^o_2$	101378	986.405	3.66E+06	2.67E-03
$3s\,7s\,^3S_1$	$3s\,3p\,^3P^o_0$	101230	987.846	6.99E+06	3.07E-03
$3s\,7s\,^3S_1$	$3s\,3p\,^3P^o_1$	101171	988.416	2.10E+07	9.23E-03
$3s\,7s\,^3S_1$	$3s\,3p\,^3P^o_2$	101048	989.621	3.51E+07	1.55E-02
$3s\,5d\,^3D_1$	$3s\,3p\,^3P^o_0$	95568	1046.369	2.20E+07	1.08E-02
$3s\,5d\,^3D_1$	$3s\,3p\,^3P^o_1$	95510	1047.009	1.64E+07	8.06E-03
$3s\,5d\,^3D_2$	$3s\,3p\,^3P^o_1$	95509	1047.015	2.95E+07	2.42E-02
$3s\,5d\,^3D_3$	$3s\,3p\,^3P^o_2$	95390	1048.321	3.87E+07	4.46E-02
$3s\,5d\,^3D_1$	$3s\,3p\,^3P^o_2$	95387	1048.360	1.08E+06	5.32E-04
$3s\,5d\,^3D_2$	$3s\,3p\,^3P^o_2$	95386	1048.366	9.69E+06	7.98E-03
$3s\,6s\,^3S_1$	$3s\,3p\,^3P^o_0$	94941	1053.280	1.30E+07	6.51E-03
$3s\,6s\,^3S_1$	$3s\,3p\,^3P^o_1$	94883	1053.928	3.92E+07	1.96E-02
$3s\,6s\,^3S_1$	$3s\,3p\,^3P^o_2$	94760	1055.298	6.54E+07	3.28E-02
$3s\,4d\,^1D_2$	$3s\,3p\,^3P^o_1$	87545	1142.262	1.18E+04	1.15E-05
$3s\,4d\,^3D_1$	$3s\,3p\,^3P^o_0$	84240	1187.083	8.09E+07	5.13E-02
$3s\,4d\,^3D_1$	$3s\,3p\,^3P^o_1$	84181	1187.907	6.04E+07	3.83E-02
$3s\,4d\,^3D_2$	$3s\,3p\,^3P^o_1$	84180	1187.921	1.09E+08	1.15E-01
$3s\,4d\,^3D_3$	$3s\,3p\,^3P^o_2$	84061	1189.600	1.44E+08	2.13E-01
$3s\,4d\,^3D_1$	$3s\,3p\,^3P^o_2$	84058	1189.646	3.99E+06	2.54E-03
$3s\,4d\,^3D_2$	$3s\,3p\,^3P^o_2$	84057	1189.661	3.59E+07	3.81E-02

Table 11: Continued.

Upper	Lower	ΔE (cm^{-1})	λ (Å)	A(s^{-1})	gf
$3s5s\ ^3S_1$	$3s3p\ ^3P^o_0$	82813	1207.528	2.78E+07	1.83E-02
$3s5s\ ^3S_1$	$3s3p\ ^3P^o_1$	82755	1208.380	8.36E+07	5.49E-02
$3s5s\ ^3S_1$	$3s3p\ ^3P^o_2$	82632	1210.180	1.40E+08	9.21E-02
$3s6d\ ^1D_2$	$3s3p\ ^1P^o_1$	79515	1257.622	9.85E+07	1.17E-01
$3s7s\ ^1S_0$	$3s3p\ ^1P^o_1$	78991	1265.955	3.54E+07	8.51E-03
$3p^2\ ^1S_0$	$3s3p\ ^3P^o_1$	74582	1340.798	6.89E+04	1.86E-05
$3s5d\ ^1D_2$	$3s3p\ ^1P^o_1$	74160	1348.418	2.24E+08	3.05E-01
$3s6s\ ^1S_0$	$3s3p\ ^1P^o_1$	72971	1370.399	6.44E+07	1.81E-02
$3s3d\ ^1D_2$	$3s3p\ ^3P^o_2$	72703	1375.454	1.72E+04	2.44E-05
$3s4d\ ^1D_2$	$3s3p\ ^1P^o_1$	65066	1536.881	6.38E+08	1.13E+00
$3s5s\ ^1S_0$	$3s3p\ ^1P^o_1$	61561	1624.379	1.47E+08	5.80E-02
$3s3p\ ^1P^o_1$	$3s^2\ ^1S_0$	59982	1667.153	1.40E+09	1.76E+00
$3s3d\ ^3D_1$	$3s3p\ ^3P^o_0$	58349	1713.817	6.66E+08	8.80E-01
$3s3d\ ^3D_1$	$3s3p\ ^3P^o_1$	58290	1715.533	5.02E+08	6.65E-01
$3s3d\ ^3D_2$	$3s3p\ ^3P^o_1$	58287	1715.635	8.98E+08	1.98E+00
$3s3d\ ^3D_3$	$3s3p\ ^3P^o_2$	58178	1718.862	1.20E+09	3.71E+00
$3s3d\ ^3D_1$	$3s3p\ ^3P^o_2$	58167	1719.164	3.37E+07	4.48E-02
$3s3d\ ^3D_2$	$3s3p\ ^3P^o_2$	58164	1719.266	3.02E+08	6.69E-01
$3s4s\ ^1S_0$	$3s3p\ ^3P^o_1$	58039	1722.962	1.46E+05	6.50E-05
$3p3d\ ^1D^o_2$	$3p^2\ ^1D_2$	57272	1746.051	1.22E+09	2.78E+00
$3p^2\ ^3P_2$	$3s3p\ ^3P^o_1$	56871	1758.350	3.15E+08	7.29E-01
$3p^2\ ^3P_1$	$3s3p\ ^3P^o_0$	56819	1759.960	4.15E+08	5.78E-01
$3p^2\ ^3P_1$	$3s3p\ ^3P^o_1$	56761	1761.771	3.06E+08	4.27E-01
$3p^2\ ^3P_2$	$3s3p\ ^3P^o_2$	56748	1762.164	9.26E+08	2.16E+00
$3p^2\ ^3P_0$	$3s3p\ ^3P^o_1$	56707	1763.431	1.24E+09	5.76E-01
$3p^2\ ^3P_1$	$3s3p\ ^3P^o_2$	56637	1765.600	5.17E+08	7.25E-01
$3p3d\ ^3F^o_2$	$3p^2\ ^1D_2$	55923	1788.172	1.27E+06	3.05E-03
$3s7p\ ^3P^o_2$	$3p^2\ ^1D_2$	54579	1832.189	6.52E+02	1.64E-06
$3s7p\ ^3P^o_1$	$3p^2\ ^1D_2$	54575	1832.327	1.23E+04	1.85E-05
$3s7p\ ^1P^o_1$	$3p^2\ ^1D_2$	54455	1836.350	3.38E+07	5.13E-02
$3s4s\ ^3S_1$	$3s3p\ ^3P^o_0$	53980	1852.525	8.61E+07	1.33E-01
$3s4s\ ^3S_1$	$3s3p\ ^3P^o_1$	53921	1854.531	2.56E+08	3.95E-01
$3s4s\ ^3S_1$	$3s3p\ ^3P^o_2$	53798	1858.774	4.17E+08	6.49E-01
$3s6f\ ^1F^o_3$	$3p^2\ ^1D_2$	53744	1860.653	7.65E+07	2.78E-01
$3s6f\ ^3F^o_3$	$3p^2\ ^1D_2$	53136	1881.932	7.13E+03	2.65E-05
$3s6f\ ^3F^o_2$	$3p^2\ ^1D_2$	53117	1882.602	5.53E+04	1.47E-04
$3p^2\ ^1S_0$	$3s3p\ ^1P^o_1$	52103	1919.249	1.02E+09	5.63E-01
$3s3d\ ^1D_2$	$3s3p\ ^1P^o_1$	50347	1986.192	1.39E+09	4.10E+00
$3s6p\ ^3P^o_1$	$3p^2\ ^1D_2$	49493	2020.447	2.12E+05	3.90E-04
$3s6p\ ^1P^o_1$	$3p^2\ ^1D_2$	49440	2022.650	3.56E+07	6.54E-02
$3s7p\ ^3P^o_2$	$3s4s\ ^3S_1$	48846	2047.233	1.08E+06	3.40E-03
$3s7p\ ^3P^o_1$	$3s4s\ ^3S_1$	48842	2047.405	1.15E+06	2.17E-03
$3s7p\ ^3P^o_0$	$3s4s\ ^3S_1$	48841	2047.456	1.17E+06	7.34E-04
$3p3d\ ^1D^o_2$	$3p^2\ ^3P_1$	48699	2053.390	6.45E+04	2.04E-04
$3p^2\ ^1D_2$	$3s3p\ ^3P^o_1$	48188	2075.166	1.79E+04	5.78E-05
$3s5f\ ^1F^o_3$	$3p^2\ ^1D_2$	48174	2075.798	1.32E+08	5.99E-01
$3p^2\ ^1D_2$	$3s3p\ ^3P^o_2$	48065	2080.480	2.83E+04	9.17E-05
$3s5f\ ^3F^o_3$	$3p^2\ ^1D_2$	47952	2085.405	2.44E+04	1.12E-04
$3p3d\ ^3F^o_3$	$3p^2\ ^3P_2$	47289	2114.616	1.50E+04	7.04E-05
$3p3d\ ^1D^o_2$	$3s3d\ ^3D_2$	47173	2119.831	3.77E+04	1.27E-04
$3p3d\ ^1D^o_2$	$3s3d\ ^3D_1$	47170	2119.987	2.33E+05	7.85E-04
$3p3d\ ^1D^o_2$	$3s3d\ ^3D_3$	47159	2120.446	4.83E+04	1.63E-04
$3s7p\ ^3P^o_1$	$3p^2\ ^3P_0$	46056	2171.238	6.16E+03	1.31E-05
$3s7p\ ^3P^o_2$	$3p^2\ ^3P_1$	46007	2173.566	1.95E+03	6.89E-06
$3s7p\ ^3P^o_1$	$3p^2\ ^3P_1$	46003	2173.760	7.16E+03	1.52E-05
$3s7p\ ^3P^o_0$	$3p^2\ ^3P_1$	46002	2173.817	2.55E+04	1.81E-05

Table 11: Continued.

Upper	Lower	ΔE (cm^{-1})	λ (Å)	A(s^{-1})	gf
$3p\,3d\,^3F^o_4$	$3s\,3d\,^3D_3$	45963	2175.649	3.79E+08	2.42E+00
$3s\,7p\,^3P^o_2$	$3p^2\,^3P_2$	45896	2178.795	1.20E+04	4.26E-05
$3s\,7p\,^3P^o_1$	$3p^2\,^3P_2$	45892	2178.991	9.08E+03	1.94E-05
$3p\,3d\,^3F^o_3$	$3s\,3d\,^3D_2$	45873	2179.885	3.17E+08	1.58E+00
$3p\,3d\,^3F^o_3$	$3s\,3d\,^3D_3$	45860	2180.536	4.10E+07	2.05E-01
$3p\,3d\,^3F^o_2$	$3s\,3d\,^3D_2$	45824	2182.239	5.58E+07	1.99E-01
$3p\,3d\,^3F^o_2$	$3s\,3d\,^3D_1$	45821	2182.404	2.96E+08	1.06E+00
$3p\,3d\,^3F^o_2$	$3s\,3d\,^3D_3$	45810	2182.891	1.63E+06	5.84E-03
$3s\,7p\,^3P^o_1$	$3s\,4s\,^1S_0$	44724	2235.899	5.78E+03	1.30E-05
$3s\,7p\,^1P^o_1$	$3s\,4s\,^1S_0$	44605	2241.891	2.19E+07	4.96E-02
$3s\,7p\,^3P^o_2$	$3s\,3d\,^3D_2$	44480	2248.152	1.01E+04	3.82E-05
$3s\,7p\,^3P^o_2$	$3s\,3d\,^3D_1$	44477	2248.328	7.31E+02	2.77E-06
$3s\,7p\,^3P^o_1$	$3s\,3d\,^3D_2$	44476	2248.361	4.46E+04	1.01E-04
$3s\,7p\,^3P^o_1$	$3s\,3d\,^3D_1$	44473	2248.536	1.57E+04	3.56E-05
$3s\,7p\,^3P^o_0$	$3s\,3d\,^3D_1$	44472	2248.597	5.95E+04	4.51E-05
$3s\,7p\,^3P^o_2$	$3s\,3d\,^3D_3$	44467	2248.845	4.99E+04	1.89E-04
$3s\,6f\,^3F^o_3$	$3p^2\,^3P_2$	44454	2249.502	4.93E+03	2.62E-05
$3s\,6p\,^3P^o_2$	$3s\,4s\,^3S_1$	43767	2284.814	5.09E+05	1.99E-03
$3s\,6p\,^3P^o_1$	$3s\,4s\,^3S_1$	43760	2285.144	5.43E+05	1.28E-03
$3s\,6p\,^3P^o_0$	$3s\,4s\,^3S_1$	43758	2285.292	5.59E+05	4.38E-04
$3s\,6f\,^3F^o_4$	$3s\,3d\,^3D_3$	43057	2322.466	1.92E+07	1.40E-01
$3s\,6f\,^3F^o_3$	$3s\,3d\,^3D_2$	43038	2323.510	1.91E+07	1.08E-01
$3s\,6f\,^3F^o_3$	$3s\,3d\,^3D_3$	43024	2324.250	2.54E+06	1.44E-02
$3s\,6f\,^3F^o_2$	$3s\,3d\,^3D_2$	43019	2324.532	3.76E+06	1.52E-02
$3s\,6f\,^3F^o_2$	$3s\,3d\,^3D_1$	43015	2324.719	1.96E+07	7.93E-02
$3s\,6f\,^3F^o_2$	$3s\,3d\,^3D_3$	43005	2325.272	1.14E+05	4.60E-04
$3s\,6p\,^3P^o_1$	$3p^2\,^3P_0$	40975	2440.496	2.47E+03	6.62E-06
$3s\,6p\,^3P^o_1$	$3p^2\,^3P_1$	40921	2443.683	2.82E+03	7.59E-06
$3s\,6p\,^3P^o_0$	$3p^2\,^3P_1$	40919	2443.852	9.55E+03	8.55E-06
$3s\,6p\,^3P^o_2$	$3p^2\,^3P_2$	40817	2449.916	4.45E+03	2.00E-05
$3s\,6p\,^3P^o_1$	$3p^2\,^3P_2$	40811	2450.296	3.19E+03	8.61E-06
$3s\,5p\,^1P^o_1$	$3p^2\,^1D_2$	40385	2476.131	4.16E+07	1.15E-01
$3s\,5p\,^3P^o_1$	$3p^2\,^1D_2$	40181	2488.690	6.83E+04	1.90E-04
$3s\,6p\,^3P^o_1$	$3s\,4s\,^1S_0$	39643	2522.492	8.39E+04	2.40E-04
$3s\,6p\,^1P^o_1$	$3s\,4s\,^1S_0$	39589	2525.927	1.56E+07	4.47E-02
$3s\,6p\,^3P^o_2$	$3s\,3d\,^3D_2$	39401	2537.958	7.58E+04	3.66E-04
$3s\,6p\,^3P^o_2$	$3s\,3d\,^3D_1$	39398	2538.181	5.13E+03	2.48E-05
$3s\,6p\,^3P^o_1$	$3s\,3d\,^3D_2$	39395	2538.364	3.62E+05	1.05E-03
$3s\,6p\,^3P^o_1$	$3s\,3d\,^3D_1$	39391	2538.588	1.22E+05	3.54E-04
$3s\,6p\,^3P^o_0$	$3s\,3d\,^3D_1$	39389	2538.769	4.82E+05	4.66E-04
$3s\,6p\,^3P^o_2$	$3s\,3d\,^3D_3$	39388	2538.839	4.15E+05	2.01E-03
$3s\,4f\,^1F^o_3$	$3p^2\,^1D_2$	37964	2634.026	2.39E+08	1.74E+00
$3s\,4f\,^3F^o_3$	$3p^2\,^1D_2$	37916	2637.386	2.65E+05	1.93E-03
$3s\,5f\,^3F^o_3$	$3s\,3d\,^3D_2$	37853	2641.745	3.01E+07	2.20E-01
$3s\,5f\,^3F^o_4$	$3s\,3d\,^3D_3$	37849	2642.057	3.44E+07	3.24E-01
$3s\,5f\,^3F^o_2$	$3s\,3d\,^3D_2$	37848	2642.131	5.14E+06	2.69E-02
$3s\,5f\,^3F^o_2$	$3s\,3d\,^3D_1$	37844	2642.373	2.80E+07	1.47E-01
$3s\,5f\,^3F^o_3$	$3s\,3d\,^3D_3$	37840	2642.700	3.69E+06	2.71E-02
$3s\,5f\,^3F^o_2$	$3s\,3d\,^3D_3$	37834	2643.087	1.44E+05	7.55E-04
$3s\,3p\,^3P^o_1$	$3s^2\,^1S_0$	37503	2666.401	3.05E+03	9.77E-06
$3s\,4s\,^1S_0$	$3s\,3p\,^1P^o_1$	35560	2812.084	3.42E+08	4.06E-01
$3s\,5p\,^3P^o_2$	$3s\,4s\,^3S_1$	34461	2901.791	7.90E+04	4.99E-04
$3s\,5p\,^3P^o_1$	$3s\,4s\,^3S_1$	34448	2902.867	6.43E+04	2.44E-04
$3s\,5p\,^3P^o_0$	$3s\,4s\,^3S_1$	34443	2903.270	5.91E+04	7.46E-05
$3p^2\,^3P_0$	$3s\,3p\,^1P^o_1$	34228	2921.510	1.01E+05	1.29E-04
$3s\,6d\,^3D_1$	$3s\,4p\,^3P^o_0$	33422	2991.956	4.17E+06	1.68E-02

Table 11: Continued.

Upper	Lower	ΔE (cm^{-1})	λ (Å)	A(s^{-1})	gf
$3s\,6d\,^3D_1$	$3s\,4p\,^3P^o_1$	33410	2993.033	3.11E+06	1.25E-02
$3s\,6d\,^3D_2$	$3s\,4p\,^3P^o_1$	33410	2993.068	5.59E+06	3.76E-02
$3s\,6d\,^3D_3$	$3s\,4p\,^3P^o_2$	33386	2995.205	7.38E+06	6.95E-02
$3s\,6d\,^3D_1$	$3s\,4p\,^3P^o_2$	33381	2995.643	2.05E+05	8.26E-04
$3s\,6d\,^3D_2$	$3s\,4p\,^3P^o_2$	33381	2995.679	1.85E+06	1.24E-02
$3s\,7s\,^3S_1$	$3s\,4p\,^3P^o_0$	33093	3021.769	2.49E+06	1.02E-02
$3s\,7s\,^3S_1$	$3s\,4p\,^3P^o_1$	33081	3022.867	7.45E+06	3.06E-02
$3s\,7s\,^3S_1$	$3s\,4p\,^3P^o_2$	33052	3025.531	1.24E+07	5.10E-02
$3p\,3d\,^1D^o_2$	$3s\,3d\,^1D_2$	32634	3064.225	9.24E+05	6.50E-03
$3s\,6d\,^1D_2$	$3s\,4p\,^1P^o_1$	32364	3089.786	1.21E+07	8.63E-02
$3s\,7s\,^1S_0$	$3s\,4p\,^1P^o_1$	31841	3140.580	2.37E+07	3.51E-02
$3s\,5p\,^3P^o_0$	$3p^2\,^3P_1$	31604	3164.071	7.97E+03	1.20E-05
$3s\,5p\,^3P^o_2$	$3p^2\,^3P_2$	31511	3173.398	4.17E+03	3.15E-05
$3s\,5p\,^3P^o_1$	$3p^2\,^3P_2$	31499	3174.685	3.15E+03	1.43E-05
$3s\,5p\,^1P^o_1$	$3s\,4s\,^1S_0$	30534	3274.939	6.31E+06	3.05E-02
$3s\,5p\,^3P^o_1$	$3s\,4s\,^1S_0$	30331	3296.944	1.47E+04	7.20E-05
$3s\,5p\,^3P^o_2$	$3s\,3d\,^3D_2$	30096	3322.700	2.84E+05	2.35E-03
$3s\,5p\,^3P^o_2$	$3s\,3d\,^3D_1$	30092	3323.083	1.90E+04	1.57E-04
$3s\,5p\,^3P^o_1$	$3s\,3d\,^3D_2$	30083	3324.111	1.39E+06	6.90E-03
$3s\,5p\,^3P^o_2$	$3s\,3d\,^3D_3$	30082	3324.212	1.58E+06	1.31E-02
$3s\,5p\,^3P^o_1$	$3s\,3d\,^3D_1$	30079	3324.494	4.63E+05	2.30E-03
$3s\,5p\,^3P^o_0$	$3s\,3d\,^3D_1$	30075	3325.021	1.84E+06	3.05E-03
$3s\,7p\,^3P^o_1$	$3s\,3d\,^1D_2$	29937	3340.241	3.62E+03	1.82E-05
$3s\,7p\,^1P^o_1$	$3s\,3d\,^1D_2$	29818	3353.632	1.16E+07	5.85E-02
$3s\,4f\,^1F^o_3$	$3p^2\,^3P_2$	29282	3415.054	1.61E+04	1.97E-04
$3s\,6f\,^1F^o_3$	$3s\,3d\,^1D_2$	29107	3435.584	3.96E+06	4.90E-02
$3s\,7p\,^1P^o_1$	$3p^2\,^1S_0$	28062	3563.501	5.99E+05	3.42E-03
$3s\,4f\,^1F^o_3$	$3s\,3d\,^3D_2$	27866	3588.582	2.31E+05	3.13E-03
$3s\,4f\,^1F^o_3$	$3s\,3d\,^3D_3$	27852	3590.346	2.88E+04	3.89E-04
$3s\,4f\,^3F^o_3$	$3s\,3d\,^3D_2$	27817	3594.822	2.10E+08	2.84E+00
$3s\,4f\,^3F^o_2$	$3s\,3d\,^3D_2$	27815	3595.101	3.67E+07	3.55E-01
$3s\,4f\,^3F^o_2$	$3s\,3d\,^3D_1$	27812	3595.550	1.98E+08	1.92E+00
$3s\,4f\,^3F^o_4$	$3s\,3d\,^3D_3$	27807	3596.091	2.36E+08	4.12E+00
$3s\,4f\,^3F^o_3$	$3s\,3d\,^3D_3$	27804	3596.592	2.61E+07	3.55E-01
$3s\,4f\,^3F^o_2$	$3s\,3d\,^3D_3$	27801	3596.871	1.05E+06	1.01E-02
$3s\,5d\,^3D_1$	$3s\,4p\,^3P^o_0$	27431	3645.449	1.30E+07	7.80E-02
$3s\,5d\,^3D_1$	$3s\,4p\,^3P^o_1$	27419	3647.047	9.74E+06	5.83E-02
$3s\,5d\,^3D_2$	$3s\,4p\,^3P^o_1$	27418	3647.118	1.75E+07	1.75E-01
$3s\,5d\,^3D_3$	$3s\,4p\,^3P^o_2$	27393	3650.450	2.33E+07	3.26E-01
$3s\,5d\,^3D_1$	$3s\,4p\,^3P^o_2$	27390	3650.926	6.45E+05	3.87E-03
$3s\,5d\,^3D_2$	$3s\,4p\,^3P^o_2$	27389	3650.997	5.81E+06	5.80E-02
$3s\,5d\,^1D_2$	$3s\,4p\,^1P^o_1$	27010	3702.264	3.33E+07	3.43E-01
$3s\,6s\,^3S_1$	$3s\,4p\,^3P^o_0$	26804	3730.736	4.80E+06	3.00E-02
$3s\,6s\,^3S_1$	$3s\,4p\,^3P^o_1$	26792	3732.410	1.44E+07	9.00E-02
$3s\,6s\,^3S_1$	$3s\,4p\,^3P^o_2$	26763	3736.471	2.39E+07	1.50E-01
$3s\,6s\,^1S_0$	$3s\,4p\,^1P^o_1$	25820	3872.818	4.27E+07	9.61E-02
$3p^2\,^1D_2$	$3s\,3p\,^1P^o_1$	25710	3889.513	2.52E+05	2.86E-03
$3s\,6p\,^3P^o_1$	$3s\,3d\,^1D_2$	24856	4023.083	6.29E+04	4.58E-04
$3s\,6p\,^1P^o_1$	$3s\,3d\,^1D_2$	24802	4031.827	1.12E+07	8.19E-02
$3s\,5f\,^1F^o_3$	$3s\,3d\,^1D_2$	23536	4248.662	6.92E+04	1.31E-03
$3s\,6p\,^3P^o_1$	$3p^2\,^1S_0$	23100	4328.924	2.63E+03	2.22E-05
$3s\,6p\,^1P^o_1$	$3p^2\,^1S_0$	23046	4339.048	4.83E+05	4.09E-03
$3s\,4p\,^1P^o_1$	$3p^2\,^1D_2$	21440	4664.114	5.84E+07	5.71E-01
$3p\,3d\,^3F^o_4$	$3s\,4d\,^3D_3$	20079	4980.211	1.58E+06	5.30E-02
$3s\,7p\,^3P^o_2$	$3s\,5s\,^3S_1$	20012	4996.755	1.70E+04	3.18E-04
$3s\,7p\,^3P^o_1$	$3s\,5s\,^3S_1$	20008	4997.781	1.45E+04	1.63E-04

Table 11: Continued.

Upper	Lower	ΔE (cm^{-1})	λ (Å)	A(s^{-1})	gf
$3s\,7p\ ^3P^o_0$	$3s\,5s\ ^3S_1$	20007	4998.083	1.36E+04	5.09E-05
$3p\,3d\ ^3F^o_3$	$3s\,4d\ ^3D_2$	19980	5004.817	1.44E+06	3.77E-02
$3p\,3d\ ^3F^o_3$	$3s\,4d\ ^3D_3$	19976	5005.892	1.71E+05	4.49E-03
$3p\,3d\ ^3F^o_2$	$3s\,4d\ ^3D_2$	19931	5017.242	2.66E+05	5.01E-03
$3p\,3d\ ^3F^o_2$	$3s\,4d\ ^3D_1$	19930	5017.501	1.44E+06	2.71E-02
$3s\,4p\ ^3P^o_1$	$3p^2\ ^1D_2$	19901	5024.661	9.23E+03	1.05E-04
$3s\,4d\ ^1D_2$	$3s\,4p\ ^3P^o_1$	19454	5140.112	1.91E+04	3.79E-04
$3s\,7p\ ^1P^o_1$	$3s\,5s\ ^1S_0$	18604	5375.179	1.15E+06	1.50E-02
$3s\,7p\ ^3P^o_2$	$3s\,4d\ ^3D_2$	18587	5379.887	9.49E+04	2.06E-03
$3s\,7p\ ^3P^o_2$	$3s\,4d\ ^3D_1$	18586	5380.185	6.36E+03	1.38E-04
$3s\,7p\ ^3P^o_1$	$3s\,4d\ ^3D_2$	18583	5381.077	4.67E+05	6.08E-03
$3s\,7p\ ^3P^o_2$	$3s\,4d\ ^3D_3$	18583	5381.129	6.18E+05	1.34E-02
$3s\,7p\ ^3P^o_1$	$3s\,4d\ ^3D_1$	18582	5381.375	1.56E+05	2.03E-03
$3s\,7p\ ^3P^o_0$	$3s\,4d\ ^3D_1$	18581	5381.726	6.19E+05	2.69E-03
$3s\,4d\ ^1D_2$	$3s\,4p\ ^1P^o_1$	17916	5581.485	9.40E+07	2.20E+00
$3p\,3d\ ^1D^o_2$	$3s\,4d\ ^1D_2$	17915	5581.778	1.04E+04	2.42E-04
$3s\,6f\ ^3F^o_4$	$3s\,4d\ ^3D_3$	17173	5822.799	1.37E+07	6.25E-01
$3s\,6f\ ^3F^o_3$	$3s\,4d\ ^3D_2$	17145	5832.567	1.20E+07	4.29E-01
$3s\,6f\ ^3F^o_3$	$3s\,4d\ ^3D_3$	17140	5834.030	1.50E+06	5.34E-02
$3s\,6f\ ^3F^o_2$	$3s\,4d\ ^3D_2$	17126	5839.003	2.07E+06	5.29E-02
$3s\,6f\ ^3F^o_2$	$3s\,4d\ ^3D_1$	17125	5839.355	1.12E+07	2.85E-01
$3s\,6f\ ^3F^o_2$	$3s\,4d\ ^3D_3$	17121	5840.470	5.89E+04	1.51E-03
$3s\,6g\ ^3G_3$	$3s\,4f\ ^3F^o_2$	16159	6188.211	2.29E+07	9.21E-01
$3s\,6g\ ^1G_4$	$3s\,4f\ ^3F^o_3$	16157	6188.938	1.45E+06	7.49E-02
$3s\,6g\ ^3G_4$	$3s\,4f\ ^3F^o_3$	16157	6188.988	2.19E+07	1.13E+00
$3s\,6g\ ^3G_3$	$3s\,4f\ ^3F^o_3$	16157	6189.038	2.00E+06	8.05E-02
$3s\,6g\ ^1G_4$	$3s\,4f\ ^3F^o_4$	16153	6190.421	1.23E+05	6.37E-03
$3s\,6g\ ^3G_5$	$3s\,4f\ ^3F^o_4$	16153	6190.440	2.49E+07	1.57E+00
$3s\,6g\ ^3G_4$	$3s\,4f\ ^3F^o_4$	16153	6190.471	1.43E+06	7.41E-02
$3s\,6g\ ^3G_3$	$3s\,4f\ ^3F^o_4$	16153	6190.521	3.18E+04	1.28E-03
$3s\,6g\ ^1G_4$	$3s\,4f\ ^1F^o_3$	16109	6207.521	2.33E+07	1.21E+00
$3s\,6g\ ^3G_4$	$3s\,4f\ ^1F^o_3$	16109	6207.571	1.57E+06	8.14E-02
$3s\,4d\ ^3D_1$	$3s\,4p\ ^3P^o_0$	16102	6210.038	6.37E+07	1.10E+00
$3s\,4d\ ^3D_1$	$3s\,4p\ ^3P^o_1$	16090	6214.677	4.77E+07	8.28E-01
$3s\,4d\ ^3D_2$	$3s\,4p\ ^3P^o_1$	16089	6215.071	8.58E+07	2.48E+00
$3s\,4d\ ^3D_3$	$3s\,4p\ ^3P^o_2$	16065	6224.681	1.14E+08	4.64E+00
$3s\,4d\ ^3D_1$	$3s\,4p\ ^3P^o_2$	16061	6225.945	3.17E+06	5.53E-02
$3s\,4d\ ^3D_2$	$3s\,4p\ ^3P^o_2$	16060	6226.344	2.85E+07	8.29E-01
$3s\,5s\ ^1S_0$	$3s\,4p\ ^3P^o_1$	15949	6269.600	2.03E+04	1.20E-04
$3s\,6d\ ^1D_2$	$3s\,4f\ ^1F^o_3$	15840	6313.012	1.86E+05	5.56E-03
$3s\,5p\ ^1P^o_1$	$3s\,3d\ ^1D_2$	15748	6349.956	1.46E+07	2.64E-01
$3s\,4p\ ^1P^o_1$	$3s\,4s\ ^3S_1$	15707	6366.499	1.45E+04	2.64E-04
$3s\,5p\ ^3P^o_1$	$3s\,3d\ ^1D_2$	15544	6433.210	2.74E+04	5.09E-04
$3s\,6d\ ^3D_3$	$3s\,4f\ ^3F^o_3$	15401	6492.942	6.60E+04	2.92E-03
$3s\,6d\ ^3D_1$	$3s\,4f\ ^3F^o_2$	15398	6494.093	8.48E+05	1.61E-02
$3s\,6d\ ^3D_2$	$3s\,4f\ ^3F^o_2$	15398	6494.261	9.43E+04	2.98E-03
$3s\,6d\ ^3D_3$	$3s\,4f\ ^3F^o_4$	15397	6494.573	7.52E+05	3.33E-02
$3s\,6d\ ^3D_2$	$3s\,4f\ ^3F^o_3$	15396	6495.177	7.51E+05	2.38E-02
$3s\,7p\ ^3P^o_1$	$3s\,4d\ ^1D_2$	15218	6570.855	5.94E+02	1.15E-05
$3s\,7p\ ^1P^o_1$	$3s\,4d\ ^1D_2$	15099	6622.876	2.26E+06	4.46E-02
$3s\,6p\ ^3P^o_2$	$3s\,5s\ ^3S_1$	14933	6696.224	2.94E+05	9.87E-03
$3s\,6p\ ^3P^o_1$	$3s\,5s\ ^3S_1$	14927	6699.059	2.80E+05	5.64E-03
$3s\,6p\ ^3P^o_0$	$3s\,5s\ ^3S_1$	14924	6700.325	2.75E+05	1.85E-03
$3s\,5s\ ^3S_1$	$3s\,4p\ ^3P^o_0$	14676	6813.521	1.23E+07	2.56E-01
$3s\,5s\ ^3S_1$	$3s\,4p\ ^3P^o_1$	14664	6819.105	3.67E+07	7.68E-01
$3s\,5s\ ^3S_1$	$3s\,4p\ ^3P^o_2$	14635	6832.678	6.12E+07	1.28E+00

Table 11: Continued.

Upper	Lower	ΔE (cm^{-1})	λ (Å)	A(s^{-1})	gf
$3s4d\,^3D_2$	$3s4p\,^1P^o_1$	14551	6872.163	1.42E+04	5.03E-04
$3s5s\,^1S_0$	$3s4p\,^1P^o_1$	14411	6938.889	9.99E+07	7.21E-01
$3s6f\,^1F^o_3$	$3s4d\,^1D_2$	14387	6950.294	1.06E+07	5.36E-01
$3s4p\,^3P^o_2$	$3s4s\,^3S_1$	14197	7043.300	5.68E+07	2.11E+00
$3s4p\,^3P^o_1$	$3s4s\,^3S_1$	14168	7057.781	5.65E+07	1.27E+00
$3s4p\,^3P^o_0$	$3s4s\,^3S_1$	14156	7063.773	5.64E+07	4.22E-01
$3s5p\,^1P^o_1$	$3p^2\,^1S_0$	13992	7146.931	3.12E+05	7.17E-03
$3s6p\,^3P^o_1$	$3s5s\,^1S_0$	13642	7330.218	1.48E+03	3.58E-05
$3s6d\,^1D_2$	$3s5p\,^3P^o_1$	13623	7340.409	2.32E+04	9.39E-04
$3s6p\,^1P^o_1$	$3s5s\,^1S_0$	13588	7359.294	3.75E+05	9.13E-03
$3s6p\,^3P^o_2$	$3s4d\,^3D_2$	13508	7402.719	1.61E+05	6.60E-03
$3s6p\,^3P^o_2$	$3s4d\,^3D_1$	13507	7403.284	1.07E+04	4.40E-04
$3s6p\,^3P^o_2$	$3s4d\,^3D_3$	13504	7405.076	9.15E+05	3.76E-02
$3s6p\,^3P^o_1$	$3s4d\,^3D_2$	13502	7406.184	7.86E+05	1.94E-02
$3s6p\,^3P^o_1$	$3s4d\,^3D_1$	13501	7406.749	2.62E+05	6.46E-03
$3s6p\,^3P^o_0$	$3s4d\,^3D_1$	13498	7408.291	1.05E+06	8.60E-03
$3s6d\,^1D_2$	$3s5p\,^1P^o_1$	13419	7451.887	1.19E+07	4.96E-01
$3s4f\,^1F^o_3$	$3s3d\,^1D_2$	13327	7503.412	5.28E+07	3.12E+00
$3s4f\,^3F^o_3$	$3s3d\,^1D_2$	13278	7530.744	5.43E+04	3.23E-03
$3s6d\,^3D_1$	$3s5p\,^3P^o_0$	13135	7612.801	4.68E+06	1.22E-01
$3s6d\,^3D_1$	$3s5p\,^3P^o_1$	13131	7615.566	3.49E+06	9.10E-02
$3s6d\,^3D_2$	$3s5p\,^3P^o_1$	13130	7615.798	6.28E+06	2.73E-01
$3s6d\,^3D_3$	$3s5p\,^3P^o_2$	13123	7620.139	8.29E+06	5.05E-01
$3s6d\,^3D_1$	$3s5p\,^3P^o_2$	13118	7622.980	2.32E+05	6.07E-03
$3s6d\,^3D_2$	$3s5p\,^3P^o_2$	13117	7623.218	2.09E+06	9.09E-02
$3s7s\,^1S_0$	$3s5p\,^3P^o_1$	13099	7633.716	2.61E+04	2.28E-04
$3s6d\,^3D_1$	$3s5p\,^1P^o_1$	12927	7735.627	5.76E+03	1.55E-04
$3s6d\,^3D_2$	$3s5p\,^1P^o_1$	12926	7735.873	1.08E+04	4.83E-04
$3s7s\,^1S_0$	$3s5p\,^1P^o_1$	12895	7754.354	1.43E+07	1.29E-01
$3s7s\,^3S_1$	$3s5p\,^3P^o_0$	12806	7808.834	1.49E+06	4.08E-02
$3s7s\,^3S_1$	$3s5p\,^3P^o_1$	12801	7811.743	4.45E+06	1.22E-01
$3s7s\,^3S_1$	$3s5p\,^3P^o_2$	12788	7819.544	7.42E+06	2.04E-01
$3s5f\,^3F^o_4$	$3s4d\,^3D_3$	11965	8357.382	4.13E+07	3.90E+00
$3s5f\,^3F^o_3$	$3s4d\,^3D_2$	11960	8360.813	3.68E+07	2.70E+00
$3s5f\,^3F^o_3$	$3s4d\,^3D_3$	11956	8363.819	4.60E+06	3.38E-01
$3s5f\,^3F^o_2$	$3s4d\,^3D_2$	11955	8364.687	6.45E+06	3.38E-01
$3s5f\,^3F^o_2$	$3s4d\,^3D_1$	11953	8365.408	3.48E+07	1.83E+00
$3s5f\,^3F^o_2$	$3s4d\,^3D_3$	11950	8367.697	1.84E+05	9.67E-03
$3s4p\,^1P^o_1$	$3s4s\,^1S_0$	11589	8628.396	3.11E+07	1.04E+00
$3s5g\,^3G_3$	$3s4f\,^3F^o_2$	10753	9299.627	6.61E+07	6.00E+00
$3s5g\,^1G_4$	$3s4f\,^3F^o_3$	10751	9301.218	2.12E+06	2.47E-01
$3s5g\,^3G_4$	$3s4f\,^3F^o_3$	10751	9301.348	6.54E+07	7.63E+00
$3s5g\,^3G_3$	$3s4f\,^3F^o_3$	10750	9301.495	5.78E+06	5.24E-01
$3s5g\,^1G_4$	$3s4f\,^3F^o_4$	10747	9304.567	1.98E+05	2.32E-02
$3s5g\,^3G_5$	$3s4f\,^3F^o_4$	10747	9304.619	7.20E+07	1.03E+01
$3s5g\,^3G_4$	$3s4f\,^3F^o_4$	10747	9304.697	4.30E+06	5.02E-01
$3s5g\,^3G_3$	$3s4f\,^3F^o_4$	10747	9304.844	9.18E+04	8.34E-03
$3s5g\,^1G_4$	$3s4f\,^1F^o_3$	10702	9343.262	7.00E+07	8.24E+00
$3s5g\,^3G_4$	$3s4f\,^1F^o_3$	10702	9343.393	2.32E+06	2.74E-01
$3s5d\,^1D_2$	$3s4f\,^1F^o_3$	10486	9536.434	3.97E+05	2.71E-02
$3s6p\,^3P^o_1$	$3s4d\,^1D_2$	10137	9864.550	9.00E+03	3.94E-04
$3s6p\,^1P^o_1$	$3s4d\,^1D_2$	10083	9917.280	1.76E+06	7.78E-02
$3s4p\,^3P^o_2$	$3s3d\,^3D_2$	9832	10170.426	2.36E+06	1.83E-01
$3s4p\,^3P^o_2$	$3s3d\,^3D_1$	9828	10174.016	1.57E+05	1.22E-02
$3s4p\,^3P^o_2$	$3s3d\,^3D_3$	9818	10184.606	1.32E+07	1.03E+00
$3s4p\,^3P^o_1$	$3s3d\,^3D_2$	9803	10200.647	1.17E+07	5.48E-01

Table 11: Continued.

Upper	Lower	ΔE (cm^{-1})	λ (Å)	A(s^{-1})	gf
$3s4p\ ^3P^o_1$	$3s3d\ ^3D_1$	9799	10204.248	3.91E+06	1.83E-01
$3s4p\ ^3P^o_0$	$3s3d\ ^3D_1$	9787	10216.780	1.56E+07	2.44E-01
$3s5d\ ^3D_3$	$3s4f\ ^3F^o_3$	9408	10628.676	1.84E+05	2.19E-02
$3s5d\ ^3D_1$	$3s4f\ ^3F^o_2$	9407	10630.257	2.33E+06	1.19E-01
$3s5d\ ^3D_2$	$3s4f\ ^3F^o_2$	9406	10630.856	2.59E+05	2.20E-02
$3s5d\ ^3D_3$	$3s4f\ ^3F^o_4$	9404	10633.049	2.13E+06	2.53E-01
$3s5d\ ^3D_2$	$3s4f\ ^3F^o_3$	9404	10633.298	2.07E+06	1.76E-01
$3s5f\ ^1F^o_3$	$3s4d\ ^1D_2$	8817	11340.980	3.48E+07	4.69E+00
$3p3d\ ^3F^o_4$	$3s5d\ ^3D_3$	8750	11427.683	7.71E+05	1.36E-01
$3p3d\ ^3F^o_3$	$3s5d\ ^3D_2$	8651	11558.342	5.95E+05	8.35E-02
$3p3d\ ^3F^o_3$	$3s5d\ ^3D_3$	8647	11563.809	7.85E+04	1.10E-02
$3p3d\ ^3F^o_2$	$3s5d\ ^3D_2$	8602	11624.825	9.38E+04	9.51E-03
$3p3d\ ^3F^o_2$	$3s5d\ ^3D_1$	8601	11625.541	5.07E+05	5.13E-02
$3s5d\ ^1D_2$	$3s5p\ ^3P^o_1$	8269	12093.317	4.89E+04	5.36E-03
$3s5d\ ^1D_2$	$3s5p\ ^1P^o_1$	8065	12398.902	2.66E+07	3.06E+00
$3s7p\ ^3P^o_2$	$3s6s\ ^3S_1$	7885	12681.794	1.94E+05	2.34E-02
$3s7p\ ^3P^o_1$	$3s6s\ ^3S_1$	7881	12688.407	1.88E+05	1.36E-02
$3s7p\ ^3P^o_0$	$3s6s\ ^3S_1$	7880	12690.355	1.85E+05	4.48E-03
$3p3d\ ^3F^o_4$	$3s5g\ ^3G_4$	7408	13498.793	1.66E+04	4.09E-03
$3p3d\ ^3F^o_4$	$3s5g\ ^3G_5$	7407	13498.957	3.40E+05	8.36E-02
$3p3d\ ^3F^o_3$	$3s5g\ ^3G_3$	7305	13688.842	2.08E+04	4.09E-03
$3p3d\ ^3F^o_3$	$3s5g\ ^3G_4$	7305	13689.160	2.99E+05	5.88E-02
$3p3d\ ^3F^o_3$	$3s5g\ ^1G_4$	7304	13689.441	1.29E+04	2.53E-03
$3s7p\ ^3P^o_2$	$3s5d\ ^3D_2$	7258	13776.458	7.56E+04	1.08E-02
$3s7p\ ^3P^o_2$	$3s5d\ ^3D_1$	7258	13777.464	5.06E+03	7.19E-04
$3p3d\ ^3F^o_2$	$3s5g\ ^3G_3$	7255	13782.192	3.19E+05	4.54E-02
$3s7p\ ^3P^o_2$	$3s5d\ ^3D_3$	7254	13784.225	4.72E+05	6.72E-02
$3s7p\ ^3P^o_2$	$3s5d\ ^3D_2$	7254	13784.263	3.72E+05	3.18E-02
$3s7p\ ^3P^o_1$	$3s5d\ ^3D_1$	7254	13785.270	1.24E+05	1.06E-02
$3s7p\ ^3P^o_0$	$3s5d\ ^3D_1$	7252	13787.569	4.93E+05	1.41E-02
$3s7p\ ^1P^o_1$	$3s6s\ ^1S_0$	7194	13899.371	1.28E+05	1.11E-02
$3s5d\ ^3D_1$	$3s5p\ ^3P^o_0$	7144	13997.231	1.56E+07	1.37E+00
$3s5d\ ^3D_1$	$3s5p\ ^3P^o_1$	7139	14006.583	1.17E+07	1.03E+00
$3s5d\ ^3D_2$	$3s5p\ ^3P^o_1$	7138	14007.623	2.10E+07	3.08E+00
$3s5d\ ^3D_3$	$3s5p\ ^3P^o_2$	7130	14024.655	2.79E+07	5.77E+00
$3s5d\ ^3D_1$	$3s5p\ ^3P^o_2$	7126	14031.681	7.77E+05	6.88E-02
$3s5d\ ^3D_2$	$3s5p\ ^3P^o_2$	7126	14032.724	6.99E+06	1.03E+00
$3s6s\ ^1S_0$	$3s5p\ ^3P^o_1$	7079	14125.271	5.50E+04	1.64E-03
$3s5d\ ^3D_1$	$3s5p\ ^1P^o_1$	6935	14418.155	2.01E+04	1.88E-03
$3s5d\ ^3D_2$	$3s5p\ ^1P^o_1$	6935	14419.257	3.70E+04	5.77E-03
$3s6s\ ^1S_0$	$3s5p\ ^1P^o_1$	6875	14543.953	3.05E+07	9.66E-01
$3s6s\ ^3S_1$	$3s5p\ ^3P^o_0$	6517	15344.060	3.53E+06	3.74E-01
$3s6s\ ^3S_1$	$3s5p\ ^3P^o_1$	6512	15355.299	1.06E+07	1.12E+00
$3s6s\ ^3S_1$	$3s5p\ ^3P^o_2$	6499	15385.468	1.76E+07	1.88E+00
$3s6s\ ^3S_1$	$3s5p\ ^1P^o_1$	6308	15851.352	1.84E+04	2.08E-03
$3s6g\ ^3G_3$	$3s5f\ ^3F^o_2$	6127	16320.802	1.48E+07	4.15E+00
$3s6g\ ^1G_4$	$3s5f\ ^3F^o_3$	6121	16334.878	1.10E+06	3.95E-01
$3s6g\ ^3G_4$	$3s5f\ ^3F^o_3$	6121	16335.225	1.41E+07	5.07E+00
$3s6g\ ^3G_3$	$3s5f\ ^3F^o_3$	6121	16335.545	1.30E+06	3.64E-01
$3s6g\ ^1G_4$	$3s5f\ ^3F^o_4$	6112	16359.463	8.02E+04	2.90E-02
$3s6g\ ^3G_5$	$3s5f\ ^3F^o_4$	6112	16359.597	1.62E+07	7.16E+00
$3s6g\ ^3G_4$	$3s5f\ ^3F^o_4$	6112	16359.811	9.34E+05	3.37E-01
$3s6g\ ^3G_3$	$3s5f\ ^3F^o_4$	6112	16360.159	2.07E+04	5.81E-03
$3s7p\ ^1P^o_1$	$3s5d\ ^1D_2$	6005	16652.651	4.07E+05	5.07E-02
$3s6g\ ^1G_4$	$3s5f\ ^1F^o_3$	5899	16949.354	1.61E+07	6.24E+00
$3s6g\ ^3G_4$	$3s5f\ ^1F^o_3$	5899	16949.727	1.27E+06	4.90E-01

Table 11: Continued.

Upper	Lower	ΔE (cm^{-1})	λ (Å)	A(s^{-1})	gf
$3s6f\ ^3F^o_4$	$3s5d\ ^3D_3$	5845	17108.406	1.14E+07	4.51E+00
$3s5p\ ^1P^o_1$	$3s5s\ ^3S_1$	5819	17184.906	2.41E+04	3.20E-03
$3s6f\ ^3F^o_3$	$3s5d\ ^3D_2$	5816	17193.593	1.02E+07	3.17E+00
$3s6f\ ^3F^o_3$	$3s5d\ ^3D_3$	5812	17205.722	1.28E+06	3.96E-01
$3s6f\ ^3F^o_2$	$3s5d\ ^3D_2$	5797	17249.677	1.79E+06	3.99E-01
$3s6f\ ^3F^o_2$	$3s5d\ ^3D_1$	5796	17251.254	9.65E+06	2.15E+00
$3s6f\ ^3F^o_2$	$3s5d\ ^3D_3$	5793	17261.855	5.11E+04	1.14E-02
$3s6d\ ^1D_2$	$3s5f\ ^1F^o_3$	5630	17759.623	5.17E+05	1.22E-01
$3s5p\ ^3P^o_2$	$3s5s\ ^3S_1$	5628	17768.207	1.24E+07	2.92E+00
$3s5p\ ^3P^o_1$	$3s5s\ ^3S_1$	5615	17808.614	1.23E+07	1.75E+00
$3s5p\ ^3P^o_0$	$3s5s\ ^3S_1$	5610	17823.755	1.23E+07	5.83E-01
$3s6h\ ^3H^o_4$	$3s5g\ ^3G_3$	5457	18324.080	2.53E+07	1.15E+01
$3s6h\ ^1H^o_5$	$3s5g\ ^3G_4$	5457	18324.382	1.39E+07	7.68E+00
$3s6h\ ^3H^o_5$	$3s5g\ ^3G_4$	5457	18324.449	1.18E+07	6.51E+00
$3s6h\ ^3H^o_4$	$3s5g\ ^3G_4$	5457	18324.651	1.25E+06	5.64E-01
$3s6h\ ^1H^o_6$	$3s5g\ ^3G_5$	5457	18324.684	2.66E+07	1.74E+01
$3s6h\ ^1H^o_5$	$3s5g\ ^3G_5$	5457	18324.718	3.51E+05	1.94E-01
$3s6h\ ^3H^o_5$	$3s5g\ ^3G_5$	5457	18324.751	7.15E+05	3.96E-01
$3s6h\ ^1H^o_5$	$3s5g\ ^1G_4$	5457	18324.886	1.24E+07	6.88E+00
$3s6h\ ^3H^o_4$	$3s5g\ ^3G_5$	5457	18324.953	1.32E+04	5.96E-03
$3s6h\ ^3H^o_5$	$3s5g\ ^1G_4$	5457	18324.953	1.42E+07	7.85E+00
$3s6h\ ^3H^o_4$	$3s5g\ ^1G_4$	5456	18325.154	5.74E+04	2.60E-02
$3s6d\ ^3D_1$	$3s5f\ ^3F^o_2$	5366	18635.855	1.13E+06	1.76E-01
$3s6d\ ^3D_2$	$3s5f\ ^3F^o_2$	5365	18637.245	1.26E+05	3.27E-02
$3s6d\ ^3D_3$	$3s5f\ ^3F^o_3$	5365	18638.113	8.87E+04	3.23E-02
$3s6d\ ^3D_2$	$3s5f\ ^3F^o_3$	5360	18656.508	1.01E+06	2.63E-01
$3s6d\ ^3D_3$	$3s5f\ ^3F^o_4$	5356	18670.127	1.02E+06	3.75E-01
$3s6f\ ^1F^o_3$	$3s5d\ ^1D_2$	5293	18890.165	1.21E+07	4.54E+00
$3s6f\ ^1F^o_3$	$3s5g\ ^3G_4$	5077	19696.245	1.62E+04	6.58E-03
$3s6f\ ^1F^o_3$	$3s5g\ ^1G_4$	5076	19696.865	3.79E+05	1.54E-01
$3s5p\ ^1P^o_1$	$3s5s\ ^1S_0$	4533	22056.796	6.93E+06	1.52E+00
$3s6f\ ^3F^o_4$	$3s5g\ ^3G_4$	4502	22210.081	3.29E+04	2.19E-02
$3s6f\ ^3F^o_4$	$3s5g\ ^3G_5$	4502	22210.525	6.73E+05	4.48E-01
$3s6f\ ^3F^o_3$	$3s5g\ ^3G_3$	4469	22373.467	4.50E+04	2.36E-02
$3s6f\ ^3F^o_3$	$3s5g\ ^3G_4$	4469	22374.318	6.47E+05	3.40E-01
$3s6f\ ^3F^o_3$	$3s5g\ ^1G_4$	4469	22375.069	2.74E+04	1.44E-02
$3s6f\ ^3F^o_2$	$3s5g\ ^3G_3$	4450	22468.477	7.26E+05	2.75E-01
$3s5p\ ^1P^o_1$	$3s4d\ ^3D_2$	4393	22759.239	9.37E+03	2.18E-03
$3s6d\ ^1D_2$	$3s6p\ ^1P^o_1$	4364	22909.927	9.29E+06	3.65E+00
$3s5p\ ^3P^o_1$	$3s5s\ ^1S_0$	4329	23094.955	1.09E+04	2.62E-03
$3s6d\ ^1D_2$	$3s6p\ ^3P^o_1$	4311	23196.420	5.08E+04	2.05E-02
$3s5p\ ^3P^o_2$	$3s4d\ ^3D_2$	4202	23793.718	9.46E+05	4.01E-01
$3s5p\ ^3P^o_2$	$3s4d\ ^3D_1$	4201	23799.551	6.30E+04	2.68E-02
$3s5p\ ^3P^o_2$	$3s4d\ ^3D_3$	4198	23818.030	5.29E+06	2.25E+00
$3s5p\ ^3P^o_1$	$3s4d\ ^3D_2$	4190	23866.235	4.69E+06	1.20E+00
$3s5p\ ^3P^o_1$	$3s4d\ ^3D_1$	4188	23872.103	1.56E+06	4.00E-01
$3s5p\ ^3P^o_0$	$3s4d\ ^3D_1$	4184	23899.317	6.24E+06	5.34E-01
$3s6d\ ^3D_1$	$3s6p\ ^1P^o_1$	3872	25821.845	2.19E+04	6.57E-03
$3s6d\ ^3D_2$	$3s6p\ ^1P^o_1$	3872	25824.512	3.84E+04	1.92E-02
$3s7s\ ^1S_0$	$3s6p\ ^1P^o_1$	3841	26031.701	1.17E+07	1.19E+00
$3s6d\ ^3D_1$	$3s6p\ ^3P^o_0$	3821	26167.050	5.16E+06	1.59E+00
$3s6d\ ^3D_1$	$3s6p\ ^3P^o_1$	3818	26186.374	3.84E+06	1.18E+00
$3s6d\ ^3D_2$	$3s6p\ ^3P^o_1$	3818	26189.117	6.92E+06	3.56E+00
$3s6d\ ^3D_3$	$3s6p\ ^3P^o_2$	3817	26196.115	9.23E+06	6.64E+00
$3s6d\ ^3D_1$	$3s6p\ ^3P^o_2$	3812	26229.715	2.58E+05	7.97E-02
$3s6d\ ^3D_2$	$3s6p\ ^3P^o_2$	3812	26232.467	2.31E+06	1.19E+00

Table 11: Continued.

Upper	Lower	ΔE (cm^{-1})	λ (Å)	A(s^{-1})	gf
$3s\,7s\ ^1S_0$	$3s\,6p\ ^3P^o_1$	3787	26402.222	6.55E+04	6.85E-03
$3s\,7s\ ^3S_1$	$3s\,6p\ ^1P^o_1$	3542	28225.226	2.24E+04	8.03E-03
$3s\,7s\ ^3S_1$	$3s\,6p\ ^3P^o_0$	3491	28638.114	1.32E+06	4.87E-01
$3s\,7s\ ^3S_1$	$3s\,6p\ ^3P^o_1$	3489	28661.261	3.94E+06	1.46E+00
$3s\,7s\ ^3S_1$	$3s\,6p\ ^3P^o_2$	3482	28713.272	6.59E+06	2.44E+00
$3s\,3d\ ^1D_2$	$3s\,4p\ ^1P^o_1$	3197	31278.053	5.81E+05	4.26E-01
$3s\,6p\ ^3P^o_2$	$3s\,6s\ ^3S_1$	2806	35636.395	3.83E+06	3.65E+00
$3s\,6p\ ^3P^o_1$	$3s\,6s\ ^3S_1$	2799	35716.837	3.79E+06	2.17E+00
$3s\,6p\ ^3P^o_0$	$3s\,6s\ ^3S_1$	2796	35752.720	3.80E+06	7.28E-01
$3p\,3d\ ^3F^o_4$	$3s\,6d\ ^3D_3$	2757	36259.999	3.88E+06	6.88E+00
$3s\,6p\ ^1P^o_1$	$3s\,6s\ ^3S_1$	2745	36417.932	2.03E+04	1.21E-02
$3p\,3d\ ^3F^o_3$	$3s\,6d\ ^3D_2$	2660	37592.006	3.28E+06	4.87E+00
$3p\,3d\ ^3F^o_3$	$3s\,6d\ ^3D_3$	2654	37667.053	4.14E+05	6.16E-01
$3p\,3d\ ^3F^o_2$	$3s\,6d\ ^3D_2$	2610	38304.490	5.59E+05	6.15E-01
$3p\,3d\ ^3F^o_2$	$3s\,6d\ ^3D_1$	2610	38310.360	3.02E+06	3.32E+00
$3p\,3d\ ^3F^o_2$	$3s\,6d\ ^3D_3$	2605	38382.412	1.61E+04	1.78E-02
$3s\,6p\ ^3P^o_1$	$3s\,6s\ ^1S_0$	2232	44788.821	1.17E+04	1.06E-02
$3s\,6p\ ^3P^o_2$	$3s\,5d\ ^3D_2$	2179	45880.820	3.87E+05	6.10E-01
$3s\,6p\ ^3P^o_2$	$3s\,5d\ ^3D_1$	2179	45891.979	2.58E+04	4.07E-02
$3s\,6p\ ^1P^o_1$	$3s\,6s\ ^1S_0$	2178	45896.824	1.95E+06	1.85E+00
$3s\,6p\ ^3P^o_2$	$3s\,5d\ ^3D_3$	2175	45967.290	2.16E+06	3.42E+00
$3s\,6p\ ^3P^o_1$	$3s\,5d\ ^3D_2$	2173	46014.246	1.91E+06	1.82E+00
$3s\,6p\ ^3P^o_1$	$3s\,5d\ ^3D_1$	2172	46025.470	6.36E+05	6.06E-01
$3s\,6p\ ^3P^o_0$	$3s\,5d\ ^3D_1$	2169	46085.285	2.55E+06	8.12E-01
$3s\,6p\ ^1P^o_1$	$3s\,5d\ ^3D_2$	2119	47184.723	9.97E+03	9.98E-03
$3p\,3d\ ^3F^o_4$	$3s\,6g\ ^3G_4$	2001	49963.277	3.51E+04	1.18E-01
$3p\,3d\ ^3F^o_4$	$3s\,6g\ ^3G_5$	2001	49965.274	7.45E+05	2.51E+00
$3s\,4f\ ^3F^o_3$	$3s\,4d\ ^3D_2$	1924	51959.659	3.28E+05	9.29E-01
$3s\,4f\ ^3F^o_4$	$3s\,4d\ ^3D_3$	1924	51971.000	3.70E+05	1.35E+00
$3s\,4f\ ^3F^o_2$	$3s\,4d\ ^3D_2$	1922	52018.040	5.72E+04	1.16E-01
$3s\,4f\ ^3F^o_2$	$3s\,4d\ ^3D_1$	1921	52045.925	3.09E+05	6.27E-01
$3s\,4f\ ^3F^o_3$	$3s\,4d\ ^3D_3$	1920	52075.739	4.07E+04	1.16E-01
$3p\,3d\ ^3F^o_3$	$3s\,6g\ ^3G_3$	1898	52670.944	4.54E+04	1.32E-01
$3p\,3d\ ^3F^o_3$	$3s\,6g\ ^3G_4$	1898	52674.550	6.29E+05	1.83E+00
$3p\,3d\ ^3F^o_3$	$3s\,6g\ ^1G_4$	1898	52678.158	5.13E+04	1.49E-01
$3p\,3d\ ^3F^o_2$	$3s\,6g\ ^3G_3$	1849	54080.363	6.98E+05	1.53E+00
$3s\,7p\ ^3P^o_2$	$3s\,7s\ ^3S_1$	1596	62637.411	1.51E+06	4.44E+00
$3s\,7p\ ^3P^o_1$	$3s\,7s\ ^3S_1$	1592	62799.081	1.50E+06	2.66E+00
$3s\,7p\ ^3P^o_0$	$3s\,7s\ ^3S_1$	1591	62846.836	1.50E+06	8.86E-01
$3s\,4d\ ^1D_2$	$3s\,4f\ ^1F^o_3$	1391	71840.113	1.50E+05	5.78E-01
$3s\,7p\ ^3P^o_2$	$3s\,6d\ ^3D_2$	1267	78917.878	1.81E+05	8.43E-01
$3s\,7p\ ^3P^o_2$	$3s\,6d\ ^3D_1$	1266	78943.421	1.21E+04	5.64E-02
$3s\,7p\ ^3P^o_1$	$3s\,6d\ ^3D_2$	1263	79175.310	8.96E+05	2.53E+00
$3s\,7p\ ^3P^o_1$	$3s\,6d\ ^3D_1$	1262	79200.393	2.98E+05	8.42E-01
$3s\,7p\ ^3P^o_2$	$3s\,6d\ ^3D_3$	1261	79249.350	1.02E+06	4.79E+00
$3s\,7p\ ^3P^o_0$	$3s\,6d\ ^3D_1$	1261	79275.737	1.19E+06	1.12E+00
$3s\,7p\ ^1P^o_1$	$3s\,7s\ ^1S_0$	1174	85157.115	6.48E+05	2.11E+00
$3s\,6p\ ^3P^o_1$	$3s\,5d\ ^1D_2$	1043	95859.815	1.99E+03	8.20E-03
$3s\,5p\ ^1P^o_1$	$3s\,4d\ ^1D_2$	1028	97191.175	1.30E+05	5.54E-01
$3s\,6p\ ^1P^o_1$	$3s\,5d\ ^1D_2$	989	101083.616	3.08E+05	1.42E+00
$3s\,6g\ ^3G_3$	$3s\,6f\ ^3F^o_2$	955	104605.793	2.58E+05	2.97E+00
$3s\,6g\ ^1G_4$	$3s\,6f\ ^3F^o_3$	937	106687.151	1.87E+04	2.87E-01
$3s\,6g\ ^3G_4$	$3s\,6f\ ^3F^o_3$	937	106701.949	2.32E+05	3.56E+00
$3s\,6g\ ^3G_3$	$3s\,6f\ ^3F^o_3$	937	106716.752	2.15E+04	2.57E-01
$3s\,6g\ ^3G_5$	$3s\,6f\ ^3F^o_4$	904	110592.555	2.44E+05	4.93E+00
$3s\,6g\ ^3G_4$	$3s\,6f\ ^3F^o_4$	904	110602.340	1.41E+04	2.32E-01

Table 11: Continued.

Upper	Lower	ΔE (cm^{-1})	λ (Å)	A(s^{-1})	gf
$3s\,5g\ ^3G_3$	$3s\,5f\ ^3F^o_2$	720	138790.579	3.95E+04	7.98E-01
$3s\,5g\ ^3G_4$	$3s\,5f\ ^3F^o_3$	715	139832.760	3.79E+04	1.00E+00
$3s\,5g\ ^3G_5$	$3s\,5f\ ^3F^o_4$	706	141637.041	4.05E+04	1.34E+00
$3s\,7p\ ^1P^o_1$	$3s\,6d\ ^1D_2$	650	153645.233	1.89E+05	2.01E+00
$3s\,5f\ ^3F^o_4$	$3s\,5d\ ^3D_3$	636	157064.774	4.44E+04	1.48E+00
$3s\,5f\ ^3F^o_3$	$3s\,5d\ ^3D_2$	631	158338.083	3.83E+04	1.01E+00
$3s\,5f\ ^3F^o_2$	$3s\,5d\ ^3D_1$	625	159872.102	3.51E+04	6.72E-01
$3s\,5g\ ^1G_4$	$3s\,5f\ ^1F^o_3$	493	202695.855	1.36E+04	7.55E-01
$3s\,6g\ ^1G_4$	$3s\,6f\ ^1F^o_3$	329	303370.446	1.27E+04	1.58E+00